COST MINIMIZING ENERGY MANAGEMENT CONTROL SCHEME FOR MICROGRIDS CONSIDERING DYNAMIC ELECTRICITY PRICES

by

Levi T. Miller

A thesis submitted in partial fulfillment
of the requirements for the degree

of

MASTER OF SCIENCE

in

Electrical Engineering

Approved:

Hongjie Wang, Ph.D. Major Professor	Regan Zane, Ph.D. Committee Member
Jacob Gunther, Ph.D. Committee Member	D. Richard Cutler, Ph.D. Vice Provost of Graduate Studies

UTAH STATE UNIVERSITY
Logan, Utah

2023

ABSTRACT

Cost Minimizing Energy Management Control Scheme for Microgrids Considering Dynamic Electricity Prices

by

Levi T. Miller, Master of Science

Utah State University, 2023

Major Professor: Hongjie Wang, Ph.D.
Department: Electrical and Computer Engineering

As countries develop and technology improves, the world consumes more energy than ever before. This fact along with several other political, social, and economic factors has resulted in simultaneous energy and climate crises. Microgrids form part of the solution to both these problems by increasing renewable energy sources and making electricity generation more available and local to end users. A major obstacle to the widespread adoption of microgrids is the cost of installing locally distributed energy resources and the necessary control equipment. The research in this thesis develops cost-optimal microgrid control strategies for several utility rate schedules and pricing structures including both constant and dynamic electricity prices and demand charges. The optimal control strategy is determined by casting the microgrid and its interaction with the utility as a linear programming optimization problem. The resulting control algorithms successfully reduce operation costs in all the scenarios simulated. The magnitude of savings depends largely on the type and amount of distributed energy resources that comprise the microgrid, the location of the microgrid, and the policies of the local utility. This research also presents a discussion on accurately modeling dynamic electricity prices by simulating a distribution grid and using bus voltages as a metric for local grid health. The local grid health is used as a basis for the

instantaneous price of electricity. The results of these simulations show that bus voltages alone may not be an adequate method of determining grid health and should not be used as the sole basis for modeling dynamic electricity prices.

(86 pages)

PUBLIC ABSTRACT

Cost Minimizing Energy Management Control Scheme for Microgrids Considering Dynamic Electricity Prices

Levi T. Miller

As countries develop and technology improves, the world is using more energy than ever before. This fact along with several other political, social, and economic factors has resulted in simultaneous energy and climate crises. A partial solution to both problems is bringing clean energy sources of electricity closer to the customers who use that energy. A microgrid is a smaller version of the national electric grid where smaller electricity generators are networked with local consumers and controlled independently of the main grid. Because control of electricity sources and loads are transferred to local controllers, the flexibility with which they can be controlled increases. The research presented in this thesis optimizes microgrid control strategies that minimize operational costs and can result in microgrids becoming more affordable and more widespread. The research aims to be as versatile as possible by simulating microgrids connected to utilities with a variety of different rate schedules and pricing structures. The outcome of the research shows that using optimized control strategies lowers the operational costs of microgrids in each of the cases tested. The magnitude of savings depends largely on the type and amount of electricity sources that comprise the microgrid, the location of the microgrid, and the policies of local utilities.

CONTENTS

LIST OF TABLES

LIST OF FIGURES

ACRONYMS

EIA	Energy Information Administration
IEA	International Energy Agency
PV	photovoltaic
NREL	National Renewable Energy Laboratory
dc	direct current
ac	alternating current
EV	electric vehicle
DER	distributed energy resources
PURPA	Public Utilities Regulatory Policies Act
IPP	independent power producer
ISO	independent system operator
RTO	regional transission operator
FERC	Federal Electric Regulatory Commission
SOC	state of charge
NSRDB	National Solar Radiation Database
SLC	Salt Lake City
EPRI	Electric Power Research Institute
INL	Idaho National Laboratory
pu	per unit
ERCOT	Electric Reliability Council of Texas

CHAPTER 1

INTRODUCTION

1.1 Motivation

The world's energy market is experiencing a period of rapid growth and technological advancement. As the world's population increases and as countries around the world continue to develop and provide higher a quality of life for their citizens, the energy demand worldwide increases drastically. The United States Energy Information Administration (EIA) projects a worldwide increase in energy usage of nearly 50% from 2018 to 2050 [1].

Serving such a large increase in energy demand is a challenging problem alone, yet the difficulty of the task is exacerbated by a concurrent climate crisis brought on by the overuse of fossil fuels. The burning of fossil fuels to generate electricity is a primary contributor to greenhouse gas emissions, and according to the International Energy Agency (IEA), fossil fuels are currently the world's primary source of energy [2]. Not only must the world drastically increase its energy production, it must simultaneously revolutionize both how that energy is produced and how it is transported to end users.

In response to the simultaneous need for more energy and cleaner energy sources, the energy sector has experienced several innovations in renewable energy sources. Apata et al and other researchers have observed the innovations in renewable energy and the wider shifts in the world's energy market as being part of a fourth industrial revolution [3]. This fourth industrial revolution includes innovations in renewable energy such as the drastic decrease in the cost of photovoltaic (PV) solar generation (upwards of 80% in some sectors according to the National Renewable Energy Laboratory (NREL)), improvements and cost reductions in battery storage technology, higher penetrations of electric vehicles (EV), and updates in existing electrical grid infrastructure [4].

The advent of widespread renewable energy sources has spurred a paradigm shift in the

construction and operation of utility power systems. One such change is the shift toward electricity generation and storage being localized to the load it serves. Localized electricity generation and storage have led to an increasing number of microgrids connecting to utility power systems. A microgrid is a compartmentalized power system that can generate and/or store part or all of the energy needed for its internal loads and may or may not be connected to the utility power system.

Traditional microgrids have served local loads with energy from natural gas or diesel generators. However, in the wake of the fourth industrial revolution, microgrids are operating with increasing amounts of clean, renewable energy sources. These new microgrids can be as small as single homes with rooftop PV and battery storage or as large as university campuses or entire oceanic islands. The trend towards energy demand being served by localized renewable energy sources part of microgrids addresses both the world's increase in energy demand and the need for cleaner energy.

Despite having significant potential to majorly contribute to solving the world's energy needs and the climate crisis, barriers remain against the widespread adoption of the microgrid power system model. The most significant of these challenges, despite recent and ongoing technological innovations, is cost. The capital cost of PV panels, battery storage, and other distributed energy resources (DER) is recovered by purchasing less electricity from utilities. The more money that is saved from offsetting utility power purchases with local generation, the more cost-effective microgrids become.

Unfortunately, electricity is becoming increasingly expensive, which makes recovering the capital costs of microgrids more difficult. While rising energy demands and the need for cleaner energy sources have spurred technological innovations in renewable energy sources, growing demand for clean electricity has also caused the cost per kWh of electricity to increase. Doubly driven by a global pandemic, the price per kWh of electricity has risen nearly 80% in some areas of the U.S. since 2021 according to the U.S. Bureau of Labor Statistics [5].

The less money spent on importing electricity from utilities the more cost-effective

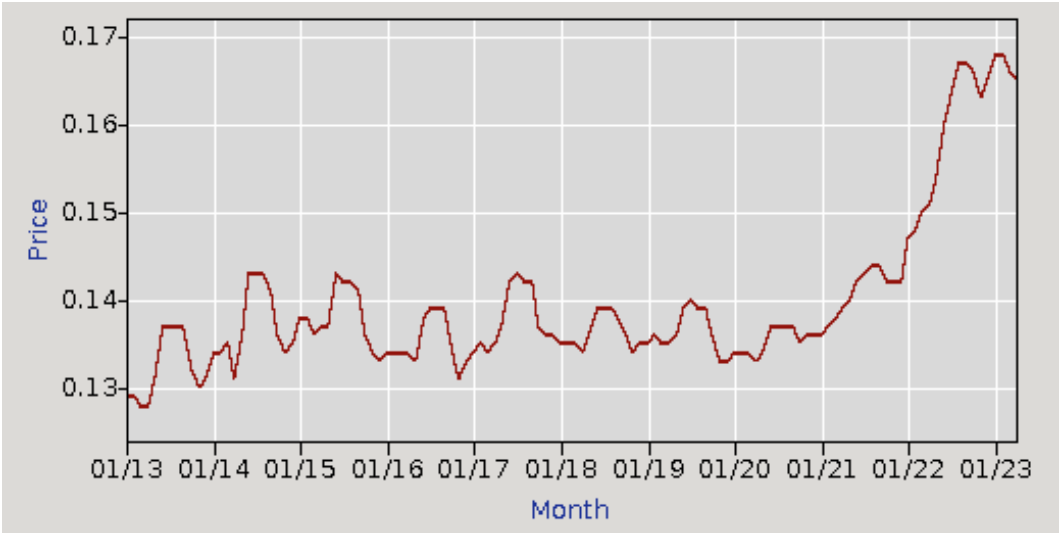

Fig. 1.1: Average Electricity Price per kWh in U.S. Cities [5].

microgrids become in addressing the world's energy needs and the fewer barriers remain against widespread microgrid adoption. The utility price of electricity cannot be directly controlled by individual customers. Consequently, reducing the costs of microgrids associated with importing electricity from utilities depends on importing as little electricity as possible. Microgrids can minimize their needed electricity imports by implementing control strategies that manage DERs more effectively and efficiently.

Many control strategies have been proposed by researchers and innovators for how to control microgrids more effectively to reduce energy import costs. A review of some of the previous research most salient to this research project will be given in the following chapter. The research presented in this thesis addresses questions centered on the interaction between microgrids and utilities which employ a dynamic pricing model. A dynamic pricing model reflects the ephemeral cost of wholesale electricity, which changes on at least an hourly basis according to complex interactions among weather patterns, demand projections, and other instantaneous conditions on the utility power system. As power systems evolve, more utilities are utilizing dynamic pricing structures. Determining a reliable method of estimating electricity prices within a reasonable margin of error when dynamic pricing structures are in place is an open research question and will be addressed in part in the

subsequent chapters.

Both dynamic electricity pricing and microgrids are becoming more common, and studying microgrids in the context of dynamic electricity pricing is an important contribution to a positive change in the world's shifting energy market. Minimizing the costs of microgrids with an optimal DER control strategy to better serve the world's evolving energy needs is the primary motivation for the research presented in this thesis.

1.2 Contents Summary

The remainder of this thesis is divided topically into the following chapters. The first (current) chapter outlined the motivation for the research and stated the problems and questions addressed by the research project. Chapter 2 contains the technical background for the study and includes a review of traditional power systems and the formation of microgrids. The technical background also outlines different types of microgrids and the traditional and emerging technologies and DERs used in microgrids. A review of various microgrid operation modes is given along with a review of research already completed on various control strategies for microgrids. The technical review concludes with an outline of how this thesis research contributes to the existing body of research.

Chapter 3 details the microgrid model used in the research. The model consists of battery storage, PV generation, local loads, and the microgrid's relationship with the utility power system, which includes traditional rate schedules and dynamic, day-ahead pricing. Each of these pieces is mathematically modeled by one or more constraint equations to be used in a linear programming optimization algorithm. Chapter 3 will also present research for a method of determining real-time electricity prices by evaluating the local health of the distribution grid. The research explores the viability of using distribution bus voltages as a metric for determining grid health and as a basis for a dynamic electricity pricing model.

Chapter 4 details the simulation design, which consists of the linear programming algorithm. Six case studies are outlined all of which use a linear programming optimization algorithm.

1. A base case using a traditional utility rate schedule
2. A scenario using dynamic electricity pricing
3. A scenario using dynamic electricity pricing with an additional demand charge component

The minimization variable in each case is the operation cost, which, for the microgrid modeled in this research, consists of the cost of imported electricity and the monthly demand charge. Chapter 4 also details the software used to implement the models, the optimization algorithm, and to run the simulations.

Chapter 5 presents the results of the case studies including a cost breakdown and a snapshot of the energy mix during the month. Chapter 6 consists of a discussion of the results and an analysis of the operational and cost differences among the case studies. Chapter 7 concludes the thesis.

CHAPTER 2
TECHNICAL BACKGROUND

2.1 Formation of Microgrids

Microgrids have been broadly defined by NREL and other research organizations as a compartmentalized power system with DER and distributed loads that can be controlled as a unit [6]. This definition states that any power system with a set of generators and loads that can be centrally controlled can be considered a microgrid regardless of the nature of the load and the source of electrical energy. This definition implies the first power systems constructed and put into service were microgrids.

Thomas Edison is widely credited with constructing the first commercially viable power system in 1882. This first power system served customers in Manhattan from a power plant on Pearl Street and generated direct current (dc) power with steam boilers fueled by burning coal [7]. Following the Pearl Street model, Edison intended to provide power everywhere with dc generators each with discrete zones of coverage. Under this model, every power system would be a microgrid, and today's power system would resemble the system depicted in figure 2.1 [8]. While more simple than modern power systems, Edison's dc power system shown in figure 2.1 lacks robustness and can only serve customers geographically near the generator.

Today's microgrids only vaguely resemble Edison's Pearl Street Station. Emerging microgrids use a wide variety of generating technologies and DERs many of which utilize renewable energy. Modern microgrids can be operated with a connection to the utility power system or independent of any other power system. In this configuration, microgrids are said to be islanded.

As the technology evolved, Edison's Pearl Street model became obsolete and the traditional power system began taking shape. The formation of the traditional power system

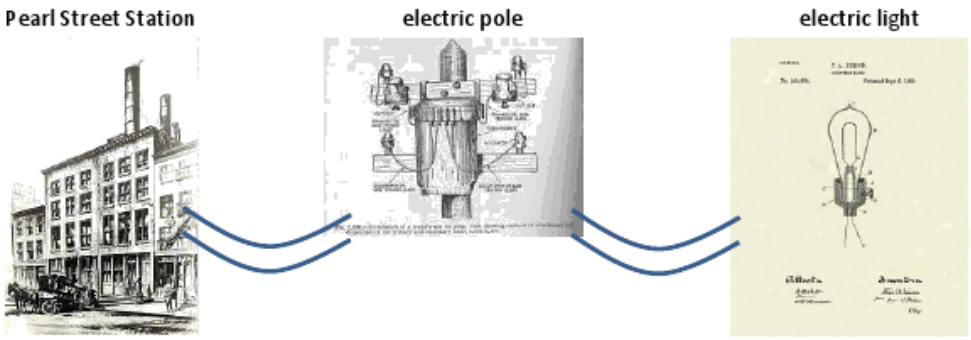

Fig. 2.1: Basic depiction of Edison's dc power system [8].

serves as the foundation of the formation of modern microgrids. Understanding why microgrids are becoming popular today requires a brief discussion of the history of the traditional power system.

2.1.1 The Traditional Power System

While Edison's Pearl Street Station was revolutionary and operated well in population-dense Manhattan, the dc power system proved to be incapable of serving the world's growing demand for energy. In the late 19th century, there was no practical way to change dc voltages. Consequently, all loads connected to a dc power system were served at the voltage produced by the generator. This voltage was often influenced by the needs of the loads and was a relatively small voltage.

Low voltages are inefficient for transporting power over anything but short distances. Ohm's law, given by (2.1), provides insight into why.

$$V = I * Z \tag{2.1}$$

According to (2.1), the voltage drop across a conductor is proportional to the current passing through the conductor and the impedance of the conductor. Thus, long conductors have high voltage drops. On a dc power system, there may not be enough voltage at the end of the line to deliver the power needed by the loads. Loads connected to the Pearl Street

Station and other similar dc power systems had to be physically close to the generator. This severely limited the versatility and scalability of early power systems.

Researchers, engineers, and entrepreneurs found a solution to this problem with the development of ac (ac) power systems. An alternating current changes in time (has a non-zero time derivative), which induces a proportional magnetic field that also changes in time. In 1873 James Clerk Maxwell published his famous paper which presented a set of equations that fully described the electromagnetic phenomenon [9]. What came to be called Maxwell's equations state that a magnetic field that changes in time will induce a proportional time-changing current in a nearby conductor [9]. These facts paved the way for the development of a machine, called a transformer, that could leverage Maxwell's equations and change the voltage of an alternating current.

Fig. 2.2: Stanley's first commercially viable transformer [11].

The first commercially practical transformer was created in 1885 by William Stanley for the Westinghouse company [10]. Stanely's original transformer is shown in figure 2.2 [11].

All transformers are based on the same electromagnetic principles first studied by Michael Faraday, and while Stanley's transformer was the first to be used in large-scale, commercially viable ac power systems, other less effective transformers were developed prior to 1885 [12]. Researchers and engineers such as Otto Blathy, Miksa Deri, Karoly Zipernowsky, and Sebastain Ferranti all developed functioning transformers of various designs and efficiencies that were all used in ac power systems [12]. Using a transformer, ac power could be changed to much higher voltages for efficient transmission to load centers great distances from generators. By the end of the 19th century, ac power systems had largely replaced dc power systems and made Edison's Pearl Street model obsolete [10].

Throughout the 20th century, ac power systems became larger in scale, more interconnected, and more reliable. By 1901, the General Electric company had developed a 500 kW turbine, which was driven by steam and fueled by coal [13]. Over one hundred years later, the largest generators have nameplate capacities upwards of 1 GW. By 2018 in the U.S. alone, the transmission network consisted of nearly 700,000 miles of transmission lines [14]. This bulk electrical system is a single network having all generators and loads connected to every other generator and load. Figure 2.3 is a depiction of the modern power system [15].

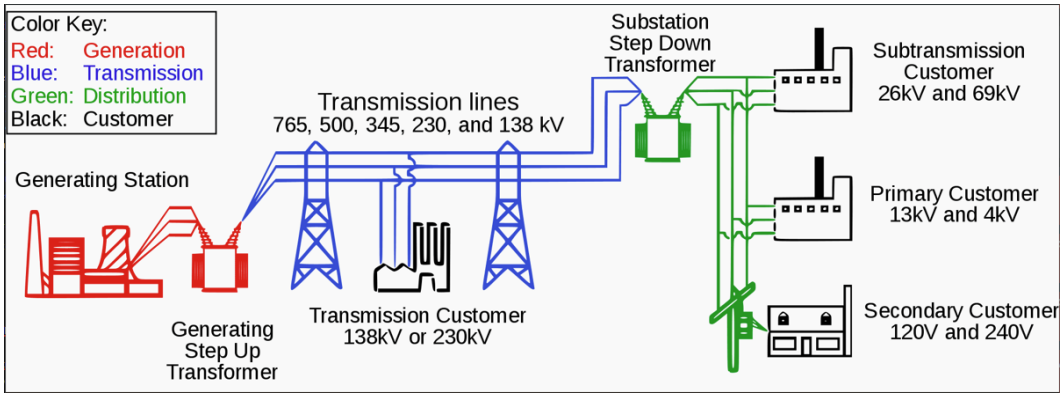

Fig. 2.3: The modern electric power system [15].

As depicted in figure 2.3, the modern power system has three main sections:

1. Generation

2. Transmission

3. Distribution

Electricity is typically generated at a few tens of kV. This is a higher voltage than Edison's Pearl Street station, but it is still inefficient to transmit electricity in this voltage range. A step-up transformer takes the voltage up to several hundreds of kV for efficient transmission. Closer to load centers, step-down transformers take the voltage down to several different voltages to serve different tiers of customers depending on their power needs.

An interconnected power system modeled in figure 2.3 has the benefit of being reliable and resilient. With Edison's Pearl Street station model, if the central generator had experienced unexpected problems or when it inevitably went into maintenance, every customer connected to the generator would have lost power. In the modern power system, each customer is connected to multiple sources of power. When one generator has problems or needs maintenance or when a power line has a problem, it is far less likely that a customer will have an outage. The evolution of power systems during the 20th century was aimed at creating larger, more reliable power systems.

While the physical implementation and theoretical paradigm of bulk electrical power systems evolved, the regulatory and policy structure of electric power systems evolved concurrently. In the U.S., a capitalist economy permitted anyone to start a power company simply by purchasing a generator, setting up distribution lines, and serving a load. This led to numerous power companies competing to serve load in small geographic areas. Situations such as the one in Vancouver shown in figure 2.4 were the result [16].

Each power company competed with other local power companies and collected customers. Each company had its own three-phase generation and distribution system. Consequently, cities began to fill with crisscrossing power lines as seen in figure 2.4. A natural solution to this problem materialized over time in the form of natural monopolies. Beginning with the Commonwealth Edison company led by Samuel Insull in Chicago, electric utilities realized that operating expenses could be lowered by increasing the load factor of their system, which is the ratio of average power usage to max power usage [17]. Systems

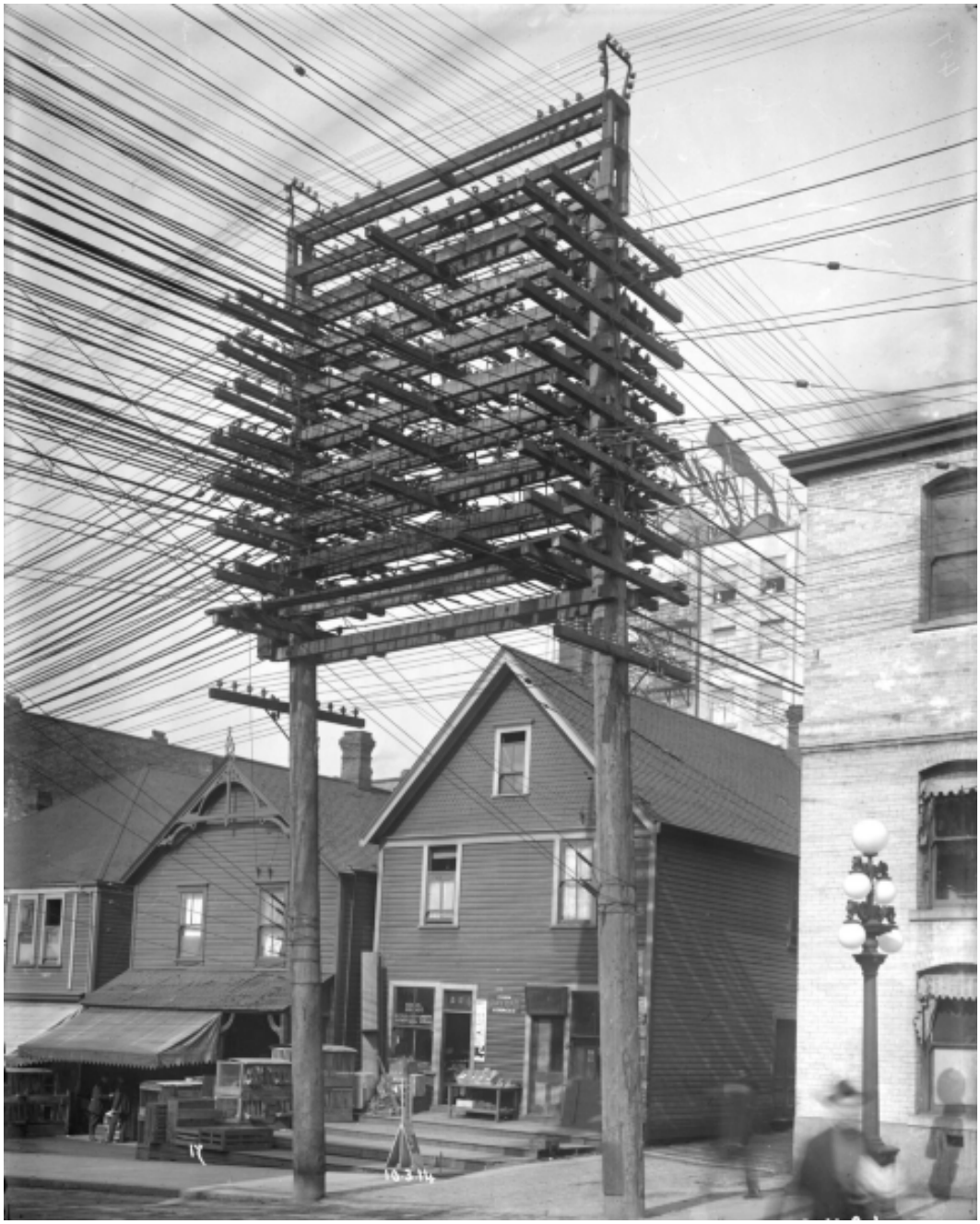

Fig. 2.4: Vancouver power lines in 1914 [16].

with a higher load factor could serve more energy with less equipment and consequently at a lower cost to consumers and a greater profit to themselves.

Electric utilities following the model set by Insull began acquiring smaller utilities to increase their customer base and more fully load their generators. In a relatively short

time, the electric power industry began to form natural monopolies. By the 1930s, only eight companies controlled 75% of the electric utility industry [18]. At this time in American history, the Progressive Era had begun. Negative experiences with monopolies created by businessmen such as Rockefeller and Carnegie caused many Americans to be distrustful of monopolies [19].

However, electric utility monopolies were not removed as people recognized having one electric power system for an area was far more efficient and safe than multiple competing utilities. A compromise was reached with legislation that created regulatory commissions for electric utilities [20]. Rate structures and new infrastructure investments were governed by public bodies while utilities retained control of electric power systems and were guaranteed no other companies would be able to operate and serve customers within their service territory. By the mid-20th century, relatively few electric utilities owned and operated the electric power system. Anyone wanting electric power had to connect to this bulk system.

The natural monopoly status of utilities began to change in the 1970s when President Carter signed the Public Utilities Regulatory Policies Act (PURPA) [21]. PURPA aimed to move the U.S. toward a more energy-efficient and energy-independent nation with several policy and regulatory changes to the energy industry. Perhaps the largest impact on electric utilities resulting from PURPA was the new requirement to purchase power from private companies producing power with privately owned generators. In the following years, independent power producers (IPP) began building generation facilities and selling power to utilities [22]. IPPs, operating independently from established monopolized utilities, began a shift in the status quo for the electric power industry. By allowing IPPs to sell power to utilities, PURPA also had the effect of spurring technological innovations in generation technology. During the late 20th century, generation technology began to diversify and improve with better gas turbines, wind power, solar cells, and geothermal generators all making entrances to national generation portfolios [22].

During the late 20th and early 21st century, the electric power industry evolved further from the changes begun with PURPA and came to include open energy markets. Across the

U.S., independent system operators (ISO) and regional transmission operators (RTO) began to form. ISOs and RTOs oversee the operation of transmission systems and the bulk electric system. Figure 2.5 shows the ISOs and RTOs currently operating in the United States. The Northwest, Southwest, and Southeast regions of the U.S. remain under vertically integrated, regulated electric utilities and have not yet developed into discrete ISOs or RTOs. ISOs and RTOs ensure a fair and open market where IPPs and utility-owned generation fleets can compete [23]. With more players in the electric power industry, regulation and cooperation became more challenging. The Federal Electric Regulatory Commission (FERC) took on responsibilities for creating and enforcing standards for operations that would ensure reliable operation of critical electrical energy infrastructure [23].

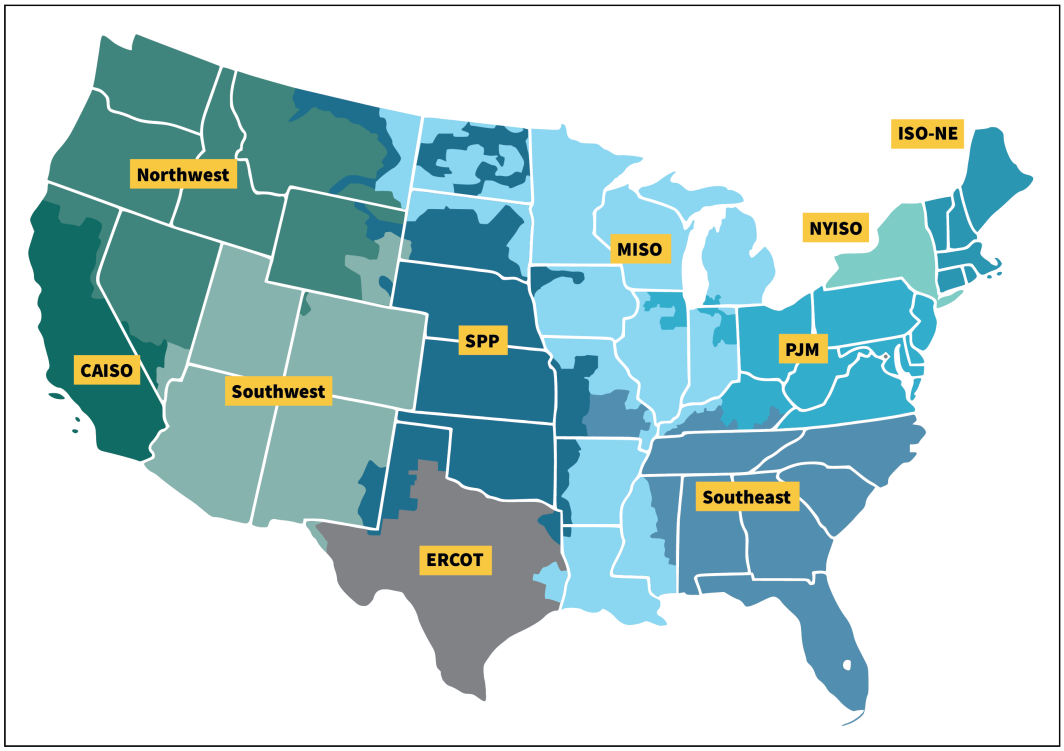

Fig. 2.5: Map of ISOs and RTOs in the U.S. [23].

During the past century, the physical implementation, business, and regulatory structure of utility power systems have evolved dramatically. Concurrently, the rate structures utilities use to bill their customers have also evolved. Before PURPA, utilities employed an

inverted rate design which charged a lower rate as customers consumed more electricity [24]. This encouraged customers to use more electricity. However, one of the actions of PURPA was to ban inverted rate structures and instead required utilities to design rate structures that would encourage the conservation of energy [21]. In the following years, utilities began employing flat rate structures or time of day and seasonal rate structures [24].

Temporally dependent rate structures charge customers different rates depending on the time of day or the time of year. Typically, electricity demand is higher in the summer when people are running air conditioning units. Under seasonal rate structures, the cost of electricity is also higher in the summer. Similarly, the demand for electricity is higher during the evening hours of the day when the most electricity is used. During these peak times, electricity is more expensive. This encourages customers to increase utility load factors by conserving energy during high-peak times and using more energy during off-peak hours.

As the complexity of power systems has grown, the variables affecting temporal rate structures have also grown. Under some ISOs where electricity markets have numerous players buying and selling power, electricity is bought and sold with prices changing as frequently as hourly. The research presented in this proposal deals specifically with these dynamic electricity prices which change on an hourly basis.

In a loose sense, the electric power industry has come full circle since its inception in the late 19th century. Beginning with the Pearl Street station model, power systems were discretely owned by independent entities and customers were served by generators close by. As power systems moved to an ac paradigm and evolved into natural monopolies and regulated, vertically integrated electric utilities, isolated cells of locally generated and consumed electricity disappeared. During the late 19th century, legislation was introduced in the U.S. that opened the doors for private companies to produce and sell power to electric utilities. As the traditional power system evolved to include open markets and numerous independent players during the early 21st century, the power system became conducive to the formation of modern microgrids.

2.1.2 Microgrid Technologies

Modern microgrids by definition include some generation and some load or loads internal to the microgrids. A microgrid may also include some form of energy storage typically using batteries. As power systems have evolved since their inception, the technologies comprising microgrids as also expanded and evolved.

Perhaps the most common microgrid generation technology is a diesel genset. A diesel genset, shown in figure 2.6, is a combination of a diesel engine and a generator [25]. Many industrial and large commercial buildings have diesel generators on site, which provide power in instances where the utility power system has an extended outage. These units are inefficient and expensive to operate as they burn expensive diesel fuel. They only operate when the utility power is off, and consequently, the microgrid does not operate in parallel to the utility power system.

Fig. 2.6: A diesel genset [25].

Another type of fossil fuel generation source used in microgrids is a natural gas turbine. Natural gas turbines, shown in figure 2.7, are often used in cogeneration facilities [26]. The

gas turbine generates heat, often in the form of steam, used to heat a single building or even an entire campus. The excess energy generated by the turbine drives a generator, which provides a part or all of the power needed by the facility [27]. Using the turbine to generate both heat and power allows it to have a higher load factor and to be used more efficiently [27].

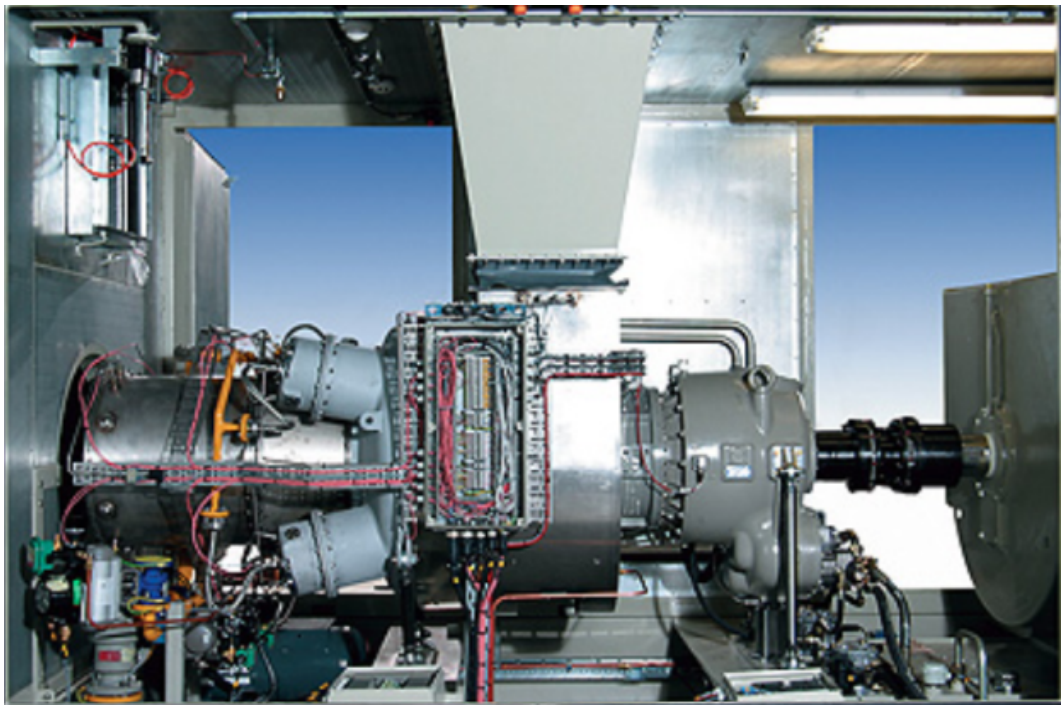

Fig. 2.7: A natural gas turbine [26].

Both diesel and natural gas generators are synchronous generators. Having a source of synchronous generation on a microgrid establishes a frequency base that inverter-based generation sources can follow [28]. Synchronous generation also helps maintain system reliability especially when microgrids are operated independently of microgrids. The nature of synchronous generators provides inertial support to microgrids, which helps balance instantaneous power and loads [28]. Because of their obvious benefits to microgrid operation, synchronous generators were among the first technologies used to build modern microgrids. As microgrids evolved, more renewable, inverter-based technologies were added to the DERs

that comprise today's microgrids.

Solar PV has become nearly ubiquitous among modern microgrids. PV panels, shown in figure 2.8, use silicon-based semiconductors to convert energy from sunlight into electricity [29]. The electricity produced by PV panels is dc, and in its native state is incompatible with consumer electronics and the bulk power system. Consequently, all power from PV is typically run through an inverter to convert the dc power to ac power before being injected into the microgrid power system. Unless specialized equipment is used, inverters convert dc power to the correct ac power by taking a frequency signal from the bulk power system or any synchronous generations also comprising the microgrid. This is another reason synchronous generators can help simplify microgrid designs. PV panels only produce power during daytime hours when the sun is shining and cannot support a microgrid power system alone.

Fig. 2.8: A PV panel [29].

The modern power grid is designed to transport power from a source to a load. It does not store energy. Electrical energy must be consumed at the same instant it is generated. Energy storage technologies allow energy to be consumed at different times than it was generated. Many different energy storage technologies exist today ranging from capacitors to pumped hydro storage. Each storage technology has different applications depending on their respective energy and power capacities [30]. Capacitors have a high power capacity

but low energy capacity. They can deliver a small amount of energy quickly making them ideal for power quality and ancillary services applications. Pumped hydro has both a high power capacity and a high energy capacity. It can serve energy for an extended period at a high power.

Batteries are the most common energy storage technology. Batteries store electric potential in the form of chemical energy. Several different chemical architectures exist for batteries, but today the best balance between energy density, power, and the cost is achieved by lithium-ion batteries. Lithium-ion batteries, shown in figure 2.9, are frequently paired with PV panels in microgrid applications to store renewable energy to be used at a later time when the PV panels are not generating power [31]. This allows microgrids to utilize renewable and relatively low-cost energy from PV panels even when the sun is not shining. Batteries also help balance generation and load within microgrids. Batteries are an easily

Fig. 2.9: A lithium-ion battery used for energy storage in microgrids [31].

dispatchable power source that can supply or consume power to balance unpredictable, instantaneous fluctuations in load or supply and maintain power system stability. Like PV panels, batteries also operate with dc power. Both of these technologies require inverters to be connected to power systems and serve typical loads.

Many other generation and storage technologies exist and are used in microgrids which are not mentioned here. This section has presented the technologies most often used in modern microgrids and most applicable to the research presented in this proposal. The theoretical microgrid which will be the subject of the research proposed later is comprised of PV panels, battery storage, and a connection to the utility power system.

2.2 Microgrid Operation

Microgrids can be operated in several different modes according to the needs and objectives of the owners and operators. One of the benefits of a microgrid is operational flexibility. Most microgrids can switch between operating modes as conditions on the power system change. Utility power systems are typically locked into a single operating mode due to their size and need to serve a diverse load base. The two main operating modes for microgrids most relevant to the research presented in this thesis are islanded operation and grid-connected operation. Figure 2.10 shows a basic schematic of a microgrid with an electrical switch that allows the microgrid to toggle between islanded and grid-connected operation [32].

2.2.1 Islanded Operation

A microgrid is said to be operating in islanded mode when it is completely disconnected and isolated from the utility power system. Thus the microgrid becomes an island from the utility power system. There are several reasons for operating in an islanded mode. In remote locations or on geographic islands, a microgrid may always operate in islanded mode because there is no utility power system with which connection is an option. Bastos and Trevizan have shown that serving remote communities with renewable energy microgrids is feasible; however, costs increase with the frequency of days with low solar output [33].

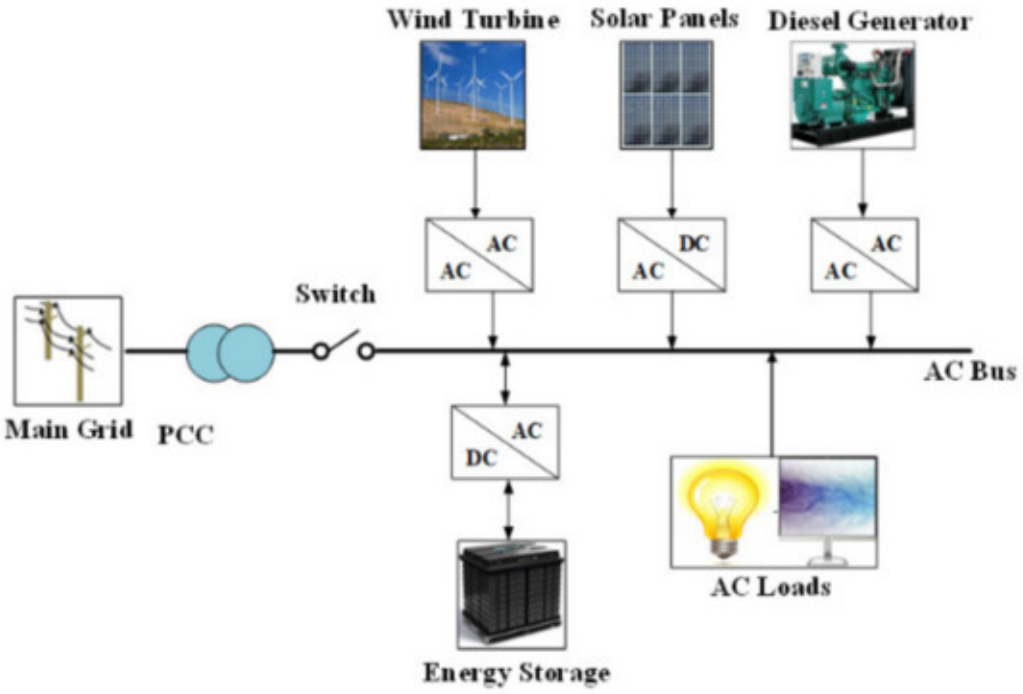

Fig. 2.10: A basic schematic of a microgrid with a disconnect switch [32].

Serving remote communities is one of the primary applications for modern microgrids.

As microgrid and DER technology improves and evolves, islanded operation for microgrids is becoming more common for microgrids that have a utility connection such as the microgrid shown in figure 2.10. These microgrids may operate in an islanded mode for reliability and power quality reasons. Sharma and associate researchers have determined a number of reliability reasons a microgrid may switch to islanded operation including:

1. Voltage unbalances
2. Voltage fluctuations
3. Intolerable frequency deviations
4. Over currents

[34]. Their team developed an algorithm for detecting conditions requiring islanded operation by monitoring the point of interconnection between the microgrid and the utility.

Operating in islanded mode for these reasons could be done to protect the microgrid from problems on the utility power system or vice versa depending on which system is currently experiencing problems.

While there are many benefits to operating microgrids in an islanded mode such as independence from the utility and the potentially eliminating utility bills, it is operationally more complex. A microgrid usually has less synchronous generation than a utility power system especially when large amounts of renewable or dc generation are present. This makes it more difficult to regulate the frequency of the system. An islanded microgrid must have a source that serves as a frequency driver for the rest of the system. This could be a synchronous generator or a large power inverter capable of forming its own frequency. Yong You and associate researchers have developed a control strategy that helps islanded microgrids regulate frequency when there is low inertial support on the system [35]. Their approach help may help alleviate some of the technological challenges with islanded microgrid operation [35].

2.2.2 Grid Connected Operation

A microgrid operates in grid-connected mode when the switch in figure 2.10 is closed. The sources on the microgrid operate in parallel with the utility power system. There are several advantages to operating a microgrid in a grid-connected. These microgrids benefit from the stability of the utility power system. Because utility power systems are large, they tend to have fewer frequency deviations and a microgrid with inverters following the utility frequency will have a more stable operation. Researchers have extensively explored the stability of grid-connected inverters. Yifeng Ouyang and Yu Zou explored improving grid-connected inverter stability using a quasi-static state inverter model and a static stability criterion [36]. Zhang and associate researchers extend the stability analysis to include multiple microgrids all with grid-connected inverters [37]. Ouyang and Zhang along with numerous other researchers have contributed to improving grid-connected inverter stability.

Grid-connected microgrids are the most common operation mode of microgrids as it is often the most simple operation mode. Operating in parallel with the utility power

system allows microgrids to utilize grid power to maintain load balance if the load exceeds local generation without curtailing load. Grid-connected operation also has the benefit of being able to export excess generation to the utility. This may introduce additional savings to the microgrid operator depending on the policies of the utility to which the microgrid is connected. In some instances, microgrids may earn a profit by selling power to the utility. Nezamabadi and Vahidasab researched a stochastic programming method to increase profits from microgrid arbitrage and make microgrid grid-connected microgrid operation more profitable [38]. However, Kadri and Raahemifar showed that the profitability of microgrid arbitrage is highly dependent on local energy market structures and utility policies [39].

The research presented in this proposal is concerned with a microgrid's interaction with a utility under different rate structures and electricity pricing. Consequently, the microgrids in this proposal are modeled as operating in a grid-connected mode.

2.3 Microgrid Control Schemes

The primary function of any power system, including microgrids, is to reliably provide power to the connected loads. However, microgrids typically have other objectives in addition to serving load. Some microgrids are operated to reduce carbon emissions, minimize energy costs, or achieve a special level of power quality. The control scheme used to operate the microgrid and schedule generation is dependent on the operational objectives of the microgrid. This section discusses two common control schemes: cost-optimized control and self-generation-optimized control.

2.3.1 Cost Optimized Control

There are two primary ways to reduce the costs of a microgrid: reducing the power purchased from the utility and extending the lifetime of equipment. Extending the lifetime of battery storage systems results in the largest cost savings. The uncertain nature of renewable energy sources tends to cause battery storage systems to charge and discharge rapidly at times. This behavior reduces the lifetime of the battery and results in expedited

equipment upgrades. Additionally, letting batteries sit at either a high or low state of charge (SOC) for long periods will also reduce the lifetime of a battery. A control scheme that extends the lifetime of battery storage systems will also reduce the costs of a microgrid.

Many researchers have worked on developing techniques for extending battery storage lifetimes and reducing the costs of operating microgrids. Researchers in the Philippines determined how to optimally size battery storage capacities to match PV arrays. [40]. When the size of the battery storage is mismatched with the PV array, uneven or frequent charging and discharging of the battery reduces the useful life of the battery storage [40]. Knöchelmann and associate researchers use conventional voltage droop curves and a particle swarm optimizer to optimize microgrid control by reducing battery storage depth of discharge, which extends the life of the battery [41]. Huang and associate researchers take the unique approach of subsidizing the energy required from the battery storage system using supercapacitors which can absorb high-frequency fluctuations in load [42]. Each of these approaches was successful in extending battery storage lifetimes and reducing microgrid costs.

Microgrids can also reduce operation costs by reducing energy expenditures. This is done most frequently by simply reducing the energy imported from the utility power system. Gupta and associate researchers developed a model of a microgrid with battery storage, PV, and a utility power system connection and showed with a simple optimized control algorithm, energy costs could be reduced [43]. Knöchelmann and associated researchers augmented the voltage droop controller with a fuzzy logic controller that was successful in both reducing microgrid operation costs as well as reducing the optimization computation time [44]. This is significant as some optimization algorithms are very time-intensive and if the computation time is too long, its output will be obsolete by the time it is available. Some researchers have developed multi-objective optimizations for reducing the costs of microgrids while also minimizing additional variables. Li and Xia developed a control algorithm to reduce microgrid costs while minimizing emissions from the microgrid [45].

2.3.2 Self-generation Optimized Control

Self-generation optimization maximizes the energy generated by the DERs connected to the microgrid. The result of self-generation optimization is practically the same as minimum cost optimization. By maximizing the energy generated by DERs, the energy imported from the grid is simultaneously minimized. For microgrids with fossil fuel generators comprising part of the energy mix, optimizing for self-generation can also reduce the fuel costs of operating local fuel generators. Headley and associate researchers developed a model for this scenario of a microgrid with renewable DERs and a diesel generator [46]. They showed that optimizing PV and battery storage systems for maximum generation can reduce microgrid costs by reducing fuel consumption of the diesel generator [46].

Zhu and associate researchers take a more general approach to self-generation optimization [47]. They use a genetic algorithm to optimize the interaction between a PV array and a battery storage system to result in the best benefit-to-cost ratio for the microgrid [47]. Bhuaneswari and associate researchers perform a similar study using an artificial immune system algorithm to optimally coordinate the various DERs in their model [48]. Their team's approach to modeling the utility power system was to feed their model a new local price of electricity every 15 minutes. This allowed the model some flexibility to adjust to changing conditions on the grid and improved their model [48].

2.4 Limitations of Existing Research

There are many aspects of microgrids, their benefits, and their integration into the existing power system that were not discussed in this chapter. There exists a plethora of research on each of these topics, and in each of these areas, there are unanswered questions and room for more research. For example, much research has been done on the optimal control of the technologies compromising microgrids, but an important question is how hundreds of small microgrids interact when networked together. How does a utility power system manage hundreds of individual residences each with a PV array and adequately sized battery storage systems? Such questions require additional consideration.

A gap in the existing research relevant to this proposal is the optimal control of microgrids when utility electricity prices are both dynamic and also known 24 hours in advance. Bhuaneswari and associate researchers study the scenario where a new electricity price is provided to the microgrid every 15 minutes ahead of when it takes effect [48]. However, the control strategy can potentially change drastically if prices are known further in advance than 15 minutes and if more than one data point is available at a time.

2.5 Proposed Contributions

As discussed in the previous section, there are gaps in the existing body of research on optimized microgrid control. The research presented in this thesis develops an algorithm and optimization model for microgrids when the hourly price of utility electricity is known 24 hours in advance. This addresses a gap in the existing body of research and complements the research done by Bhuaneswari and his team. They studied a scenario where the price of electricity at only one-time step 15 minutes in advance was available to microgrid operators [48]. Independent System Operators and other electricity market operators keep historical records of electricity prices. Consequently, it is not unreasonable to assume microgrid operators have access to historical pricing data that is a good estimate for upcoming prices. This prior knowledge can potentially change the control scheme's energy scheduling decisions in ways that may offer cost savings to microgrids.

The research presented here contributes to the existing body of research in the following ways:

1. Presents a distribution grid loading model.
2. Evaluates a method for determining grid health.
3. Develops an algorithm for cost-optimal microgrid control.
4. Implements the optimization algorithm in software.
5. Validates the optimization software.

The cost-optimal microgrid control algorithm developed in this research utilizes dynamic utility electricity prices. The dynamic utility price model is included as part of the microgrid model in chapter three and includes the presentation of research on a method of estimating real-time electricity prices by determining grid health using distribution bus voltages as a grid health metric. The dynamic electricity pricing research contributes to the existing body of research both the grid model constructed to evaluate grid health and also the conclusions drawn from the evaluation of the dynamic pricing determination method.

The proposed contributions to the existing body of research also include an algorithm for the cost-optimal control of microgrids when a dynamic utility pricing model is used. This contribution includes both the software implementation of the algorithm and microgrid model and the validation of the algorithm and model.

The research presented in this thesis models a simple microgrid consisting of solar PV, a battery storage system, and a connection to the grid. An algorithm is developed that casts the control schemes as linear programming problems and optimizes for the minimum cost of operation. The following six case studies are presented in the subsequent chapters:

1. Control optimization using a traditional, constant price rate structure.
2. Control optimization using a dynamic price rate structure.
3. Control optimization using a dynamic price rate structure with demand charge reduction included in the cost minimization.
4. Control optimization using a traditional, constant price rate structure with EV charging modeled in the microgrid load.
5. Control optimization using a dynamic price rate structure with EV charging modeled in the microgrid load.
6. Control optimization using a dynamic price rate structure with EV charging modeled in the microgrid load and demand charge reduction included in the cost minimization.

The output of the case studies is the hourly dispatch of the battery storage system and net power drawn from the grid that realizes the optimization.

CHAPTER 3
MODEL DEVELOPMENT

3.1 Model Overview

The optimization algorithm for the research question presented in this proposal is cast as a linear programming problem with time steps of an hour. Mathematical models of each component of the microgrid are needed before developing the linear programming problem. The microgrid modeled here is a relatively simple grid-connected microgrid consisting only of a PV array, a battery storage system, and a connection to the utility. The utility connection is modeled with a load balance equation. The utility rate structure varies among the cases and details will be given in the next chapter. However, each utility rate structure consists, generally, of two pieces: an energy charge and a demand charge.

3.2 Battery Energy Storage Model

Several equations are needed to adequately characterize the battery storage system. For the research presented in this proposal, the maximum charge and discharge rate of the battery storage system is equal to the size of the PV array in Watts. For this model, the batteries can charge and discharge at a maximum of 100kW. The system will use a four-hour battery storage system. This means that if the battery were fully charged and the microgrid was to draw the battery's maximum power of 100kW, the battery would last for four hours. This means the battery's energy capacity is 400 kWh. Equations 3.1 - 3.6 model the behavior of the battery storage system.

$$\text{battChar}(t) \leq 100 \tag{3.1}$$

$$\text{battDis}(t) \leq 100 \tag{3.2}$$

$$\text{SOC}(0) = 200 \tag{3.3}$$

$$\text{SOC}(t) \leq 400 \tag{3.4}$$

$$\text{SOC}(t) \geq 120 \tag{3.5}$$

$$\text{SOC}(t) = \text{SOC}(t-1) + \eta_{batt}\text{battChar}(t) - \eta_{batt}\text{battDis}(t) \tag{3.6}$$

Equations 3.1 and 3.2 set the charging and discharging power limits for the battery storage system. The battery cannot source or absorb power at a rate greater than 100kW. The terms battChar(t) and battDis(t) are the charging and discharging power respectively of the battery at hour t. When the battery is discharging, it is serving energy to the microgrid.

Equation 3.3 initializes the battery storage system to begin the simulation at 200 kWh or at 50% capacity.

Equation 3.4 sets the battery's capacity limit to 400 kWh. The battery is allowed to charge to maximum capacity. Equation 3.5 limits the battery's SOC to a minimum of 120 kWh or 30% capacity. This extends the life of the battery and is more representative of how battery storage systems are typically operated.

Equation 3.6 determines the capacity remaining in the battery at each hour where η_{batt} is the efficiency of the battery. The same efficiency is used when energy enters and leaves the battery. The battery efficiency is modeled as 90%. The SOC at hour t is determined by the SOC at the previous hour and the net power into and out of the battery during the hour. Note that equation 3.6 allows for the mathematical possibility of the battery charging and discharging at the same time. This is practically impossible. The actual power into or out of the battery during time t is determined by taking the difference between the

charging power and discharging power (battChar(t) - battDis(t)) at each hour. If the result is negative, the battery supplies power to the microgrid at hour t.

Also, note the units kW and kWh are being used somewhat interchangeably. This is allowed because the time step of the simulations is one hour, and it is assumed that power is constant over the hour. If the battery charges at 5 kW for an hour, its SOC will increase by 5 kWh. Mathematically the energy used over some time is the integral of the power used over the same interval. Using time-steps of an hour simplifies modeling equations.

3.3 PV Model

The nameplate capacity of the microgrid's PV array is 100 kW. The microgrid is modeled using solar data for the Northern Utah area. The solar data includes PV output in kW scaled up to match the size of a 100 kW array. This data was obtained using NREL's National Solar Radiation Database (NSRDB) [49]. The simulations are run over July when loading is typically highest and when solar output is also near its maximum. Only the solar data for July is used from the NSRDB solar data set. Figure **??** shows a zoomed-in portion of the solar data to show the general solar output pattern.

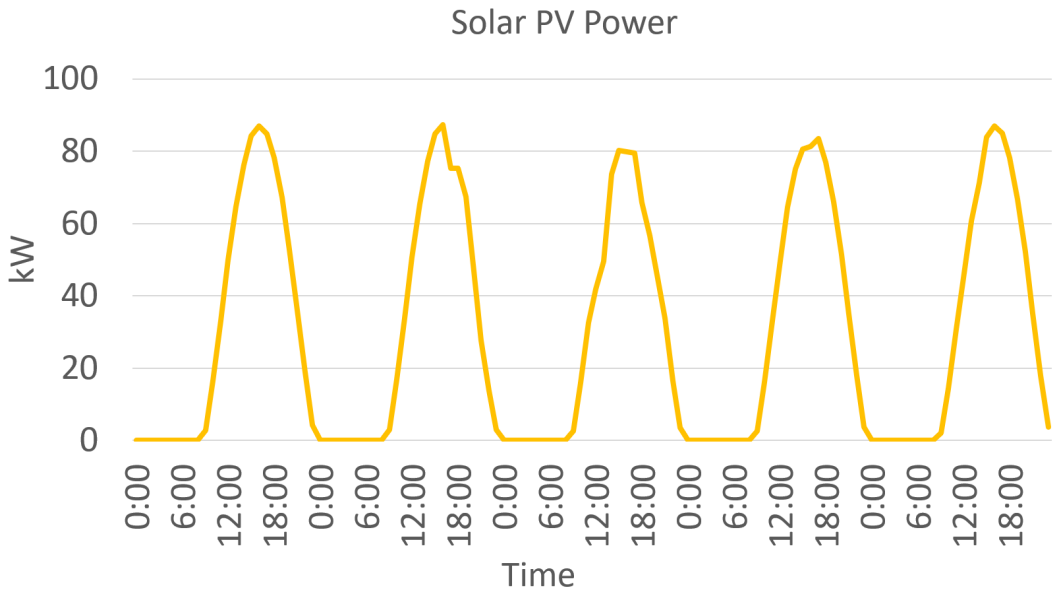

Fig. 3.1: Daily solar output pattern.

3.4 Microgrid Load Model

Two different load models are used in the microgrid model. The first is a basic load model with a typical load pattern. The second load model uses the first load model as a foundation and adds EV charging to the model.

3.4.1 Basic Load Model

The first three simulations use load data typical of average commercial loads. This data is meant to be representative of an average microgrid with loads near unity power factor. The load data is obtained from the Department of Electrical and Computer Engineering at the University of Colorado Boulder [50]. Figure 3.5 shows the load microgrid load profile and figure 3.3 shows the daily microgrid load profile.

The load profile shown in figure 3.5 is for the interval of the simulation. Figure 3.3 shows a load profile of a single day in July. Note how the load peaks during the afternoon and early evening hours and is lowest during the evening. This is typical for average load patterns.

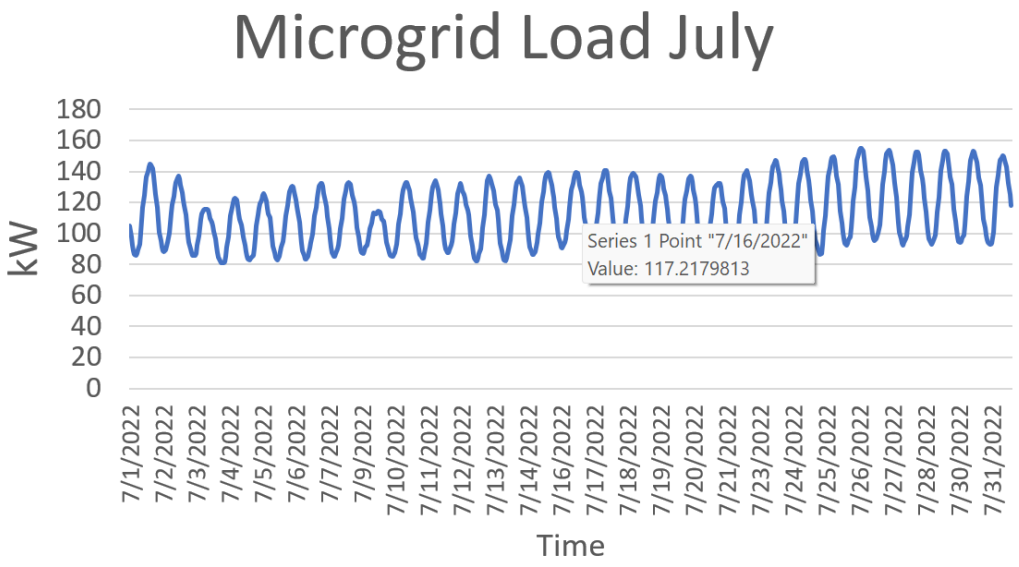

Fig. 3.2: Microgrid load profile for July.

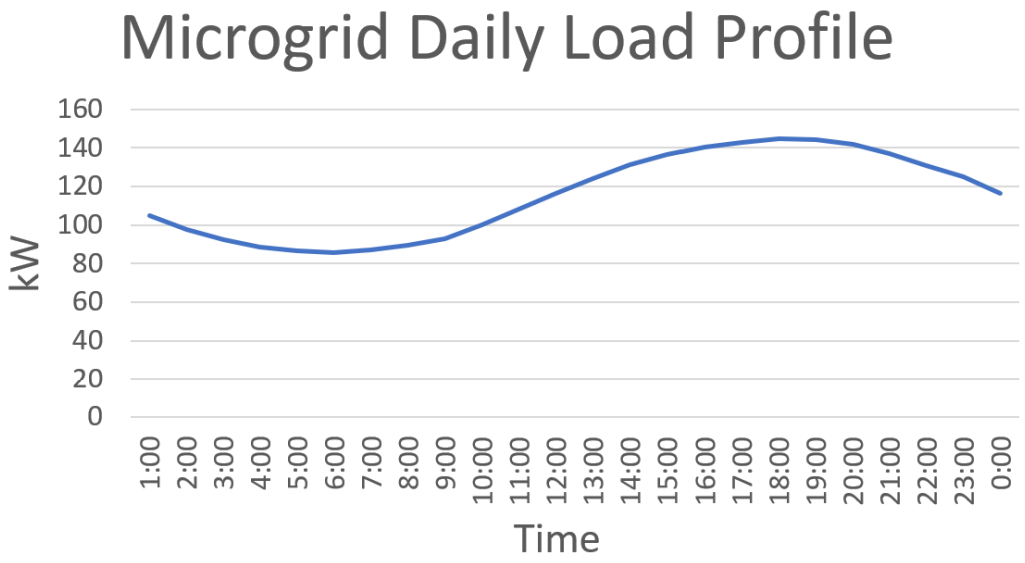

Fig. 3.3: Daily microgrid load profile.

3.4.2 Load Model with EV Charging

The final three simulations show the effect of EV charging on the microgrid. As discussed previously in this chapter, EVs are quickly increasing in popularity. EV charging will inevitably become a part of microgrid loads. Charging EVs from microgrids is less damaging to the environment as a greater part of the energy served through microgrids comes from environmentally friendly sources. Charging from a microgrid also has the potential to be less expensive than charging from the grid depending on the location and construction of the microgrid.

Modeling EV charging behavior also gives insight into how an optimal control strategy operates under large, intermittent loads. Other specialized loads may follow similar patterns to EV charging. Operators of microgrids with such loads may benefit from the results of the final three simulations.

Note that for the microgrid model to operate correctly as it has been presented, the load (or a reasonably accurate prediction) must be known in advance. The EV charging modeled here is for the scenario where EV owners schedule their charging at least 24 hours in advance with the microgrid owner. Attempting to predict EV charging load or adding a

stochastic element to the microgrid load model to more accurately predict EV charging is beyond the scope of this research.

The final three simulations use a modified version of the load profile shown in figures 3.5 and 3.3. The modified load profile is changed to model the effect of EV charging on the microgrid. For intervals of one hour, 100 kW will be drawn from the microgrid in addition to the normal load. This can model a set of vehicles simultaneously charging or one vehicle charging with a fast charger. Figure 3.4 shows a three-day snapshot of the monthly load profile used for the final three case studies.

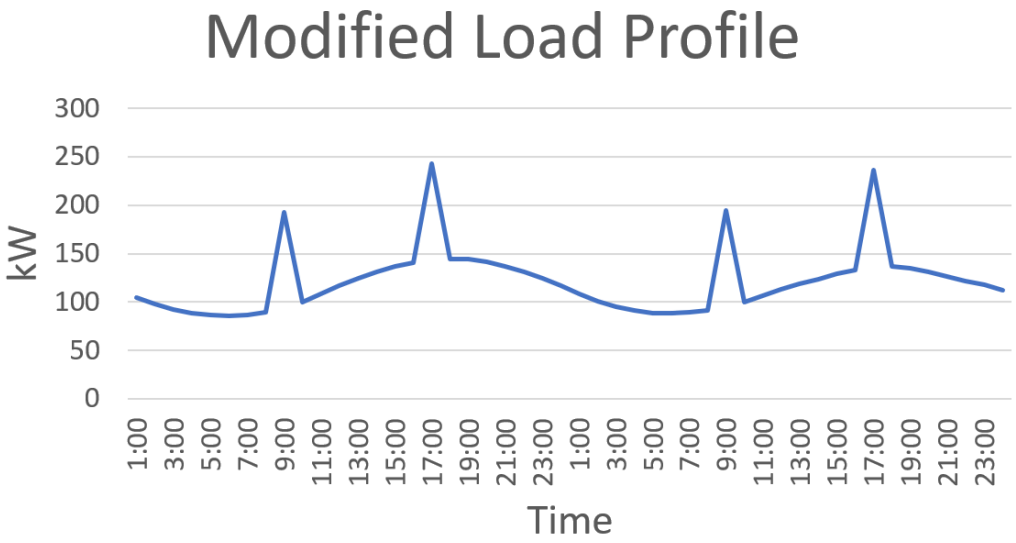

Fig. 3.4: EV load modified with EV charging.

3.5 Utility Model

Mathematically, the utility's interaction with the microgrid is modeled by equation 3.7. Equation 3.7 imposes a load balance constraint and requires the instantaneous load to be balanced with the instantaneous sum of the various power sources connected to the microgrid.

$$load(t) + \text{battChar}(t) = \text{grid}(t) + (pv(t) + \text{battDis}(t)) * \eta_{inv} \tag{3.7}$$

The terms on the left side of equation 3.7 each represent a load on the microgrid which consumes energy. Battery charging is seen as a load as it draws energy from the sources to stores for future consumption. The load term comes from the load data discussed in the previous section. The terms on the right side of equation 3.7 represent sources of energy. If the load is greater than the sum of the PV and battery storage, the load must be served partially by the grid.

Notice that the pv(t), battDis(t), and battChar(t) terms are scaled by the efficiency of the inverter. Both the battery and the PV array produce dc power, which is incompatible with microgrid loads and the utility power system. The dc power coming from the PV array and the battery storage must be changed to ac power before being used by the microgrid or passed to the utility power system. Likewise, the power coming from the grid to charge the battery must pass through the inverter. The inverter is modeled as being 90% efficient.

It is through the interaction with the utility that the microgrid accumulates costs and in some cases generates revenue. The microgrid must purchase power from the utility such that equation 3.7 is balanced. The cost of purchasing power from the utility has two parts discussed in the following sections.

3.5.1 Energy Charge

The energy charge accounts for the actual energy used by a utility customer over the billing cycle and is measured in kWh. This research models both traditional and dynamic rate schedules. For average residential and small commercial customers, the energy charge structure for a traditional rate schedule may have only a few different prices which are dependent on either the season, time of day, or both. Utilities generally have higher prices during the summer months when electricity demand is higher, and some utilities employ time-of-day pricing where prices are higher in the late afternoon and evening hours of the day when electricity demand is higher.

Dynamic energy prices are similar to time-of-day energy charge structures in that they are both driven largely by supply and demand. However, a dynamic energy charge structure, instead of only having two or three different daily prices, allows the price of electricity to

fluctuate on much more granular time steps. This allows the price of electricity to respond to more incidental stimuli such as weather or unplanned maintenance. Most days the price signal will resemble diurnal load patterns; however, the price can also fluctuate unexpectedly due to inclement weather, equipment malfunctions, or other more nebulous factors.

Energy imported from the utility is a free variable in the optimization and is used to balance the energy generated and consumed by the microgrid. At each moment, the load must be exactly balanced with energy either generated or imported from the grid. If not the microgrid will not operate correctly. The microgrid will import more energy from the grid when PV generation is low or when the control scheme decides to charge the batteries.

3.5.2 Demand Charge

Utilities must be capable of serving the maximum potential demand of their customers at any moment. However, most customers do not impose their maximum load on the grid all the time. Consequently, the utility is required to build out resources and infrastructure that are underutilized, which is not cost ineffective. To recuperate the opportunity costs of not operating the grid at maximum output, utilities include demand charges in the rate structures of large customers. The demand charge element of rate structures charges customers based on their peak demand.

Peak demand is the highest rate at which energy is required from the grid averaged over some measurement interval. For many utilities, this interval is 15 minutes [51]. Peak demand is calculated each month; therefore, a customer's highest 15-minute average demand over a month is used by the utility to calculate the demand charge. For the microgrid model used in this research, the measurement interval will be equal to the simulation time step of one hour to facilitate computational simplicity. Many utilities, charge for demand according to a rate per kW of demand [51]. In many cases, this rate is dynamic and changes depending on the tier of peak demand into which a customer falls [51]. For the research presented here, the microgrid will be charged a flat rate of $10 per kW for the peak demand over the month.

3.6 Grid Health as a Basis for Dynamic Electricity Prices

Residential and lower-power commercial customers connected to the utility power system have static rate schedules and pay the same price per kWh all the time. However, at the wholesale level, electricity prices are dynamic according to many different variables and conditions on the grid. The dynamic price of electricity can be determined by receiving a price signal directly from ISOs or other market operators, or it can be estimated by basing a price prediction on real-time grid conditions or by constructing a price prediction from historical price data. For the model presented in this proposal, dynamic electricity prices will be assumed to be close to historical prices during the same time of year and the same time of day. This greatly simplifies the model and allows more effort to be given to the main question of optimal microgrid control schemes.

The author has conducted research previously to determine the effectiveness of using real-time grid conditions to determine dynamic electricity prices. The research aimed to determine if distribution bus voltages were a viable metric for determining grid health and could serve as an effective determinant of dynamic electricity prices [52]. This research is presented here to illustrate the difficulty of determining local real-time electricity prices independently from the utility and to justify the use of historical price data in the microgrid model.

The research is presented in six sections. Section 3.6.1 presents the system model development and simulation method. Sections 3.6.2 - 3.6.4 each present a case study on how distribution bus voltages respond to different levels of EV charging on two different distribution networks. The first case study uses the IEEE 34-bus network to create a baseline of data and to test a small, weak system. The second case study uses a real distribution network from the Salt Lake City (SLC), Utah area. The third case study uses the same distribution network from SLC but with higher levels of EV charging. Section 3.6.5 presents a discussion on the results, and section 3.6.6 concludes.

3.6.1 Model Development and Simulation Method

The simulations performed in this research rely on two models:

1. The model of the EV service equipment (EVSE).

2. The distribution network OpenDSS models.

EVSE Model

The EVSE is modeled within software used under license from the Idaho National Laboratory (INL) called Caldera. Caldera takes as input the maximum power rating of each charger. To model EV charging, Caldera is given a list of EV charging sessions. The data in this list includes the type of EV charging at each charger, starting and ending charging times, starting and ending parking times, and starting and ending EV SOC. The model knows when the EV arrives, when it starts charging, when it finishes charging, and when it leaves the charger. The starting and ending SOC of the EV are input parameters for the model and, in part, dictate the power drawn by each charger. The model will charge the EV with the amount of power that is needed (within the limits of the charger) to meet the specified ending SOC in the time allotted for the charging session. The chargers used in the simulations are L2 chargers and dc fast chargers with various power ratings.

The EV charging event list for the case studies models typical public EV charging behavior. L2 chargers are often found at parking stalls in workplaces where employees park and leave their EVs plugged in for the duration of the workday. High-power dc fast chargers typically have shorter, high-power charge sessions. In this research, high-power (450 kW) dc fast charging sessions that last half an hour each and lower-power (50 kW and 150 kW) dc fast charging sessions for overnight fleet charging have been modeled for the case studies. The charge sessions are shown in Table 3.1. In each case study, each charger on the network charges an EV according to the power level of the charger and the sessions shown in Table 3.1.

Table 3.1: Charge sessions for each case study.

	L2	50 *kW*	150 *kW*	450 *kW*
Session Duration	8:00 am - 5:00 pm	1:00 am - 6:00 am	1:00 am - 6:00 am	Every 30 min 10:00 am - 8:00 pm

Distribution Network Model

The two distribution models used in this research are both modeled using the OpenDSS tool developed by the Electric Power Research Institute (EPRI):

1. the standard IEEE 34-bus system.
2. a distribution network in downtown SLC.

Both networks are radial having a single source and circuits branching off from that source. To avoid masking voltage fluctuations on the network as load changes, the load tap changers and voltage regulators in both networks were disabled for analysis and modeling. Any distributed generation (including rooftop PV) present on either network was also disabled for the power distribution network modeling.

The base load profile is the same in each case study, as shown in Fig. 3.5. This load profile contains three days of load data and is representative of a typical load profile for a distribution network. Peak loading occurs during the afternoon and evening hours and minimum loading occurs during the night. In the morning hours as the sun rises, the load begins to increase until it reaches its peak in the evening hours. The same load profile is used for all three case studies to maintain consistency and allow for better comparison between the three case studies.

Simulation Method

The system is simulated with Caldera. Caldera takes as input parameters for the EVSE model, an EV charge event list dictating how the EV chargers are utilized, a list of busses on the distribution network for which to output time-series voltage data, and the distribution network model in OpenDSS. Figure 3.6 shows a diagram for the system simulation model structure with inputs and outputs. Through Caldera, the two models work together and exchange data to generate the time-series bus voltage output.

Buses at a variety of locations on the networks are inputted to Caldera. This yields information about the effect of public EV charging on the whole distribution network instead of a single location which may not be representative of the whole network. The buses to

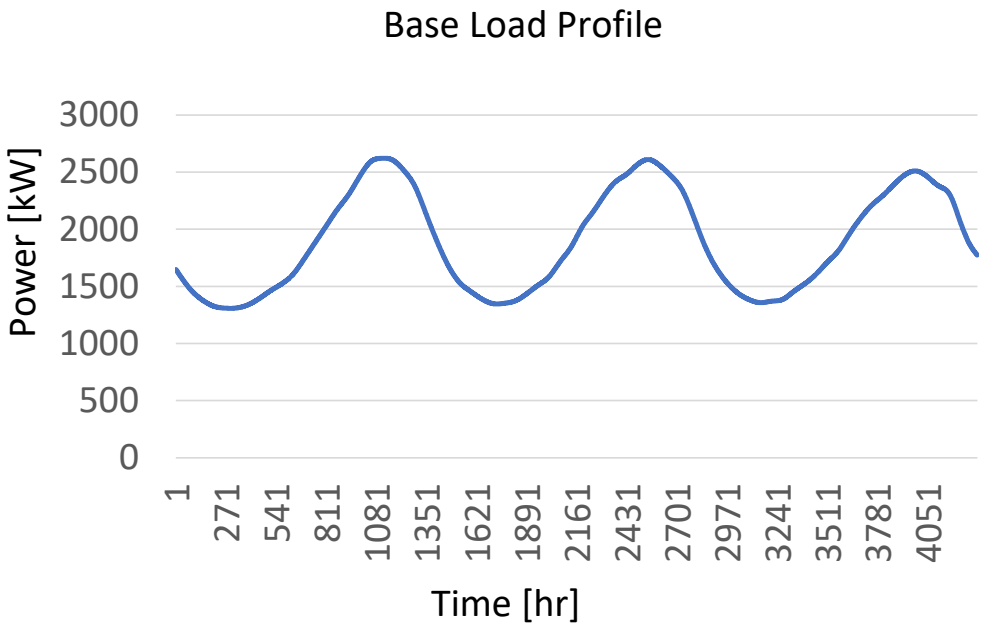

Fig. 3.5: Base load profile.

which EV chargers are connected, the source bus (substation bus), and arbitrary buses in the middle and at the end of the distribution lines are among the buses chosen to monitor. Often, voltages at the end of long distribution lines have the poorest voltage especially when no voltage regulators are present on the line. The voltage regulators in both network models have been disabled to give a clear picture of how voltage is changing in response to the EV charging loads.

Caldera provides EV charging loads to OpenDSS at each time step according to the EVSE model and the EV charge event simulation. The OpenDSS power flow for the distribution models is solved at each time step as the base load and the EV charging load change. The voltage at the chosen busses is recorded by Caldera for each time step. The outputs of the simulations include time-series voltage data for all the buses indicated in the inputs as well as time-series power data at the source for the network. These data sets give information about how power levels and voltages on the network change as a function of the base load and the EV charging load.

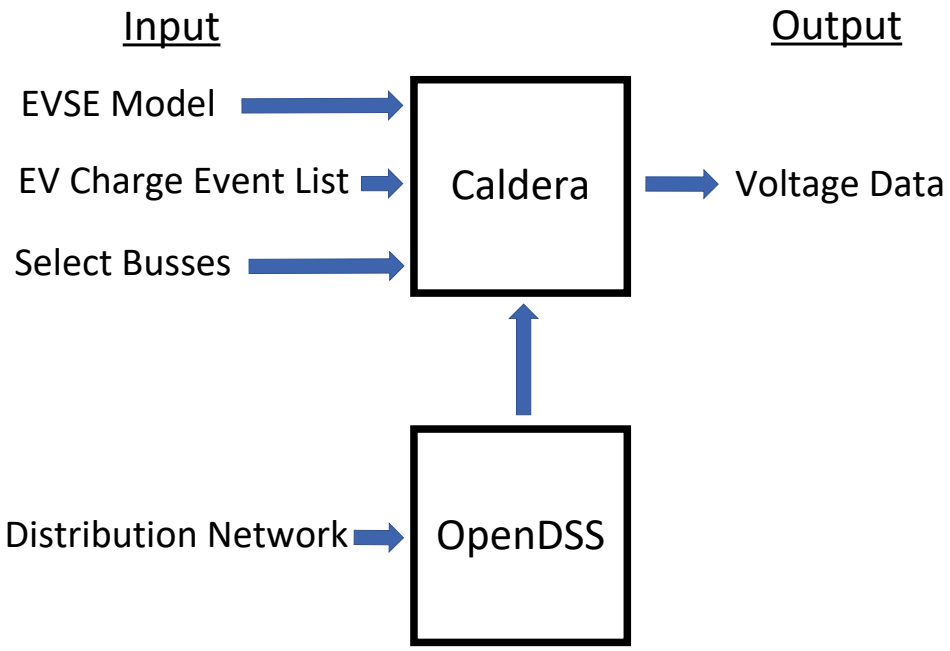

Fig. 3.6: Diagram of the system simulation method and structure.

3.6.2 IEEE 34-bus System Case Study

The first case study simulates EV charging on the IEEE 34-bus system. The results of this case study provide a baseline of data with which to compare the results of the other two case studies. The IEEE 34-bus system is a relatively simple system and any effects from EV charging on the network will be more prominent than on a bigger system with more complicated dynamics. It is also known to have very long feeders that require the application of voltage regulators to keep the voltage within bounds [53].

Model Development

The IEEE 34-bus model, shown in Fig. 3.7, has public EV charging at three locations listed in Table 3.2. The locations of buses with EV chargers are shown in Fig. 3.7. The base load for the IEEE 34-bus network has a peak value of 2621.4 kW. The base load profile shown in Fig. 3.5 is scaled by the peak load to fit the network.

Table 3.2: IEEE 34-bus system EV chargers.

	$L2$	50 kW	150 kW	450 kW
Bus 806	10	0	0	0
Bus 812	0	0	0	4
Bus 858	0	0	4	0

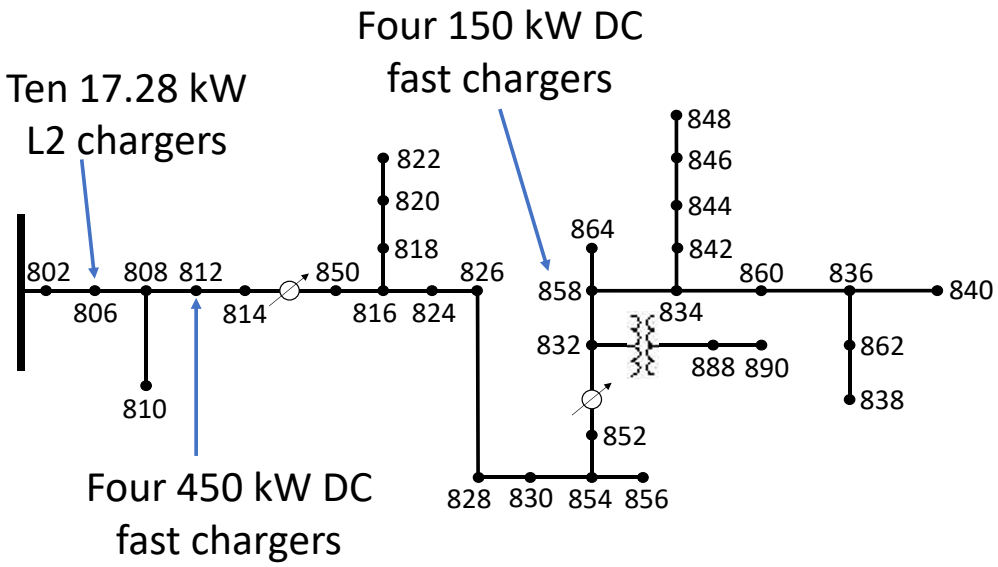

Fig. 3.7: IEEE 34-bus network.

Results

The time-series voltage data for select buses on the IEEE 34-bus network is shown in Fig. 3.8. The minimum per unit (pu) voltage defined by the National Electric code is shown as a dashed red line [54].

Figure 3.8 shows that during the morning hours of the day, despite EV charging, voltages at the buses chosen mostly stay between 1.05 pu and 1 pu. During the afternoon when the base load reaches its peak, the voltages at the buses shown in bold in Fig. 3.8 fall below the red dashed line, which is a violation of the minimum voltage limit of 0.95 pu.

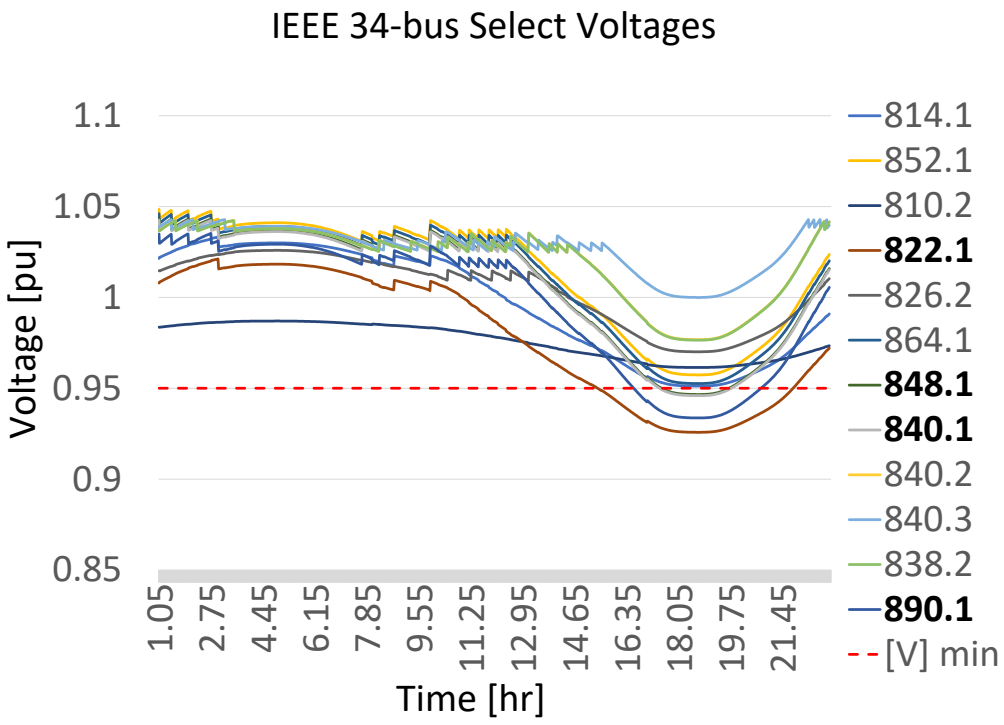

Fig. 3.8: IEEE 34-bus network select voltages.

3.6.3 SLC System Case Study

Model Development

The SLC model contains an entire distribution network starting at the substation and including the full networks of each feeder. The model includes the substation transformer and its load tap changer, voltage regulators, and time-series load data for the network. The effect of distributed solar generation is not considered in this study, and any distributed PV on the network is disabled before running the simulation.

The load profile, shown in Fig. 3.5, is scaled for this case study by the peak load seen on the SLC network on a heavily loaded summer day with a peak load of 10206.8 kW.

To remain consistent with the actual network configuration, the SLC model includes public EV charging stations at only two buses. One bus has EV charging infrastructure for both high-power electric public buses and lower-power private EVs. The other site has charging infrastructure for overnight fleet charging. These sites have been designated by the

local utility to include EV charging and development plans for the area include increasing the number of EV chargers at these locations to serve public transportation and increasing numbers of private EV charging. Table 3.3 lists the chargers at both buses with EV chargers on the SLC distribution network.

Table 3.3: SLC distribution network EV chargers.

	$L2$	50 kW	15 kW	450 kW
Bus 153	7	0	0	2
Bus 527	0	3	0	0

Besides the obvious difference in network topology, the two network models differ in relative base loading, total number of chargers, and number of charging locations. Within the limitation of the differences between the physical topology of the networks, the first two case studies use EV charging sessions chosen to load the two networks in similar ways. Loading the circuits in similar ways allows easier comparison between the two case studies.

Results

The times-series voltage data for select buses on the SLC distribution model is shown in Fig. 3.9.

During the morning hours of the day, the voltage at the buses selected stays within 1.04 and 1.03 pu except for bus 304.1. Bus 304.1 is at the end of a long distribution line and consequently has a lower voltage. During the afternoon hours when the base load reaches its peak, the voltage at the chosen buses does not fall below 1 pu. The voltage perturbations from the 30-minute charging sessions of the 450 kW dc fast chargers can be seen during the afternoon hours creating the step pattern in the voltage waveforms.

3.6.4 SLC System with High EV Loads Case Study

Model Development

Because the IEEE 34-bus system is somewhat underbuilt, voltage violations occurred

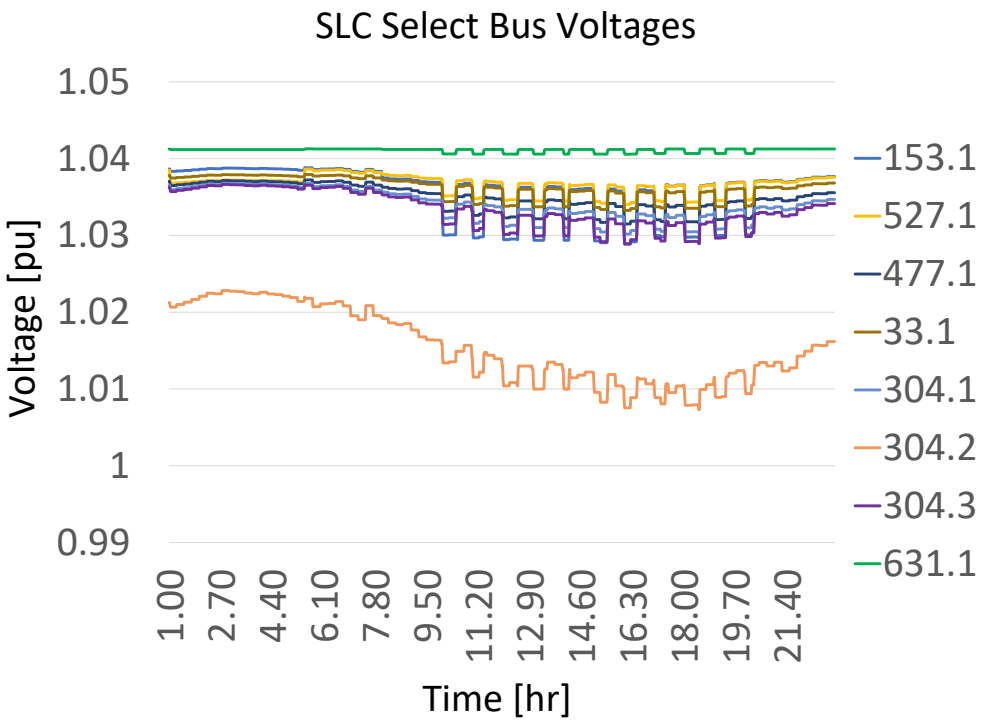

Fig. 3.9: SLC network select voltages.

with base levels of EV charging. Real distribution networks tend to be overbuilt by the utility to hedge against future growth, which is one reason no voltage violations occurred on the SLC distribution network with base levels of EV charging. The purpose of the final case study is to load the distribution network with far more EV charging to explore whether voltage violations occur when the network is loaded closer to capacity.

This study uses the SLC model with the same base loading and charging locations as in the second case study. However, the load from EV charging is adjusted to model load levels closer to the EV charging load anticipated by the local utility in the future. This is done by changing the model to include more chargers at each charging location within what is reasonable for single locations and within the plans of the utility. Thirty-five L2 chargers are modeled for this case study at bus 153 with six 450 kW dc fast chargers for public bus charging and ten 150 kW dc fast chargers for private EV charging. At bus 527, forty 150 kW dc fast chargers are included for a large fleet of EVs charging overnight. Table 3.4 shows the number of chargers at each bus for this case study.

Table 3.4: SLC distribution network with high EV charging load.

	$L2$	50 kW	150 kW	450 kW
Bus 153	35	0	10	6
Bus 527	0	40	0	0

Results

The time-series voltage data for select buses on the SLC distribution model in the case of high EV charging levels is shown in Fig. 3.10.

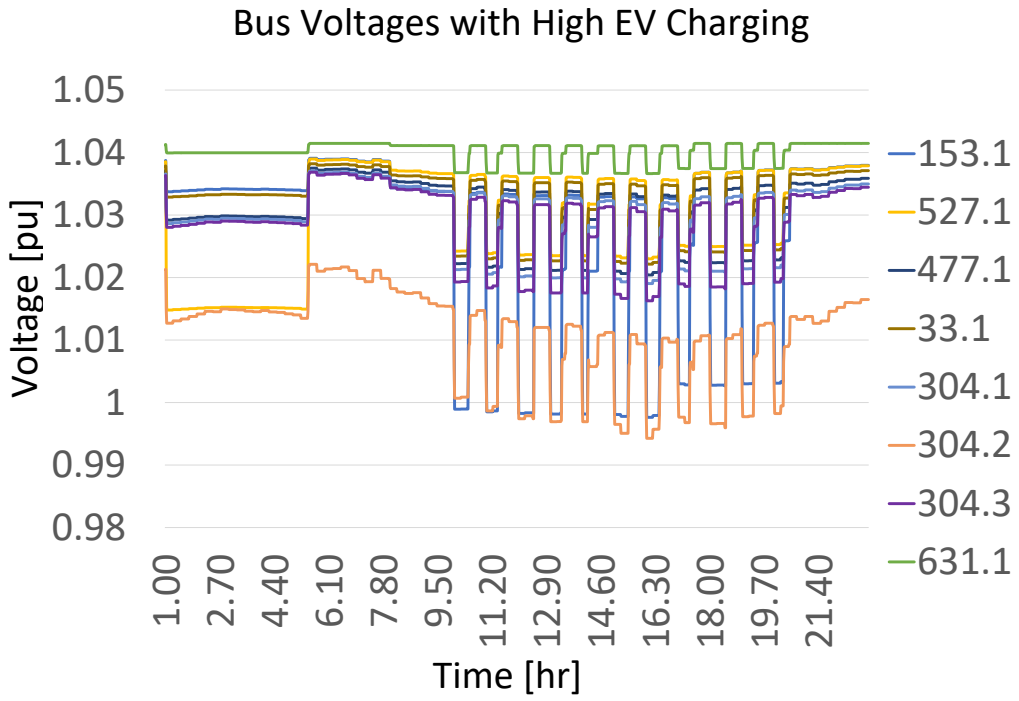

Fig. 3.10: SLC network select voltages with high EV charging.

Figure 3.10 resembles Fig. 3.9 from the second case study. In the afternoon hours when the base load reaches its peak, the voltage at the chosen busses does not fall below 0.99 pu. However, the voltage perturbations due to the 30-minute sessions of the 450 kW dc fast chargers are greater in Fig. 3.10 than in Fig. 3.9 when there is significantly more EV charging load. The voltage perturbations due to the overnight charging are also greater in Fig. 3.10.

3.6.5 Analysis

In each case study, the voltage at each of the chosen busses begins near or above 1 pu and is within tolerances specified by the National Electric Code, which restricts distribution bus voltages to 5% above or below 1 pu [54]. If the voltage exceeds 1.05 pu or falls below 0.95 pu, the voltage is out of tolerance. The voltage waveforms during the afternoon hours for the second and third case studies are more jagged compared to the first case study due, in part, to the differences in network topology between the two distribution models.

The most salient result of the case studies is the voltage violation that occurred during the first case study on the IEEE 34-bus system. The voltage falls below 0.95 pu during the peak loading hours of the day. This voltage violation is an indication that distribution bus voltages may be a metric that can be used to determine the health of the grid in the presence of EV charging. An EV charger control loop using distribution bus voltages as a control signal would raise the price of EV charging upon seeing bus voltages fall below 0.95 pu to encourage charging at different locations or different times. However, the IEEE 34-bus model may not adequately represent a real distribution network.

The IEEE 34-bus model is much smaller than a typical distribution network, which is obvious when the IEEE 34-bus system's 34 buses are compared to the SLC distribution model's 657 buses. Additionally, while the base load profiles for the three case studies were identical, the relative loading was higher on the SLC distribution model. Intuitively, higher base loading would tend to exacerbate voltage perturbations due to EV charging. However, as seen in Fig. 3.9, no voltage violations occurred on the SLC distribution network during the second case study despite both higher base loading and similar EV charging load compared to the first case study. The lack of voltage violations on the SLC distribution network during the second case study indicates the effects of widespread public EV charging on distribution networks may not be effectively simulated with standard IEEE systems, particularly on a distribution network as weak as the IEEE-34 test system.

The absence of voltage violations on the SLC distribution network during the second case study also indicates distribution bus voltages alone may not be an effective metric of

grid health. As the load increased during peak hours in the second case study, the voltage did not fall below 1 pu. If a control signal for EV charging were to be generated based on distribution bus voltages from the second case study, the price would remain constant despite the grid becoming more loaded. One reason no voltage violations were seen in the first simulation of the SLC distribution model is that utilities often overbuild distribution networks to accommodate future growth, which makes load fluctuations less impactful on distribution bus voltages.

The third case study explored the case where high levels of EV charging occurred on the SLC distribution network. This was done to study the effect of high EV charging on a system loaded closer to its capacity. As seen in Fig. 3.10, even with a significantly greater EV charging load, no voltage violations occurred. The voltages do not drop below 0.99 pu and stay above the minimum limit. While the voltage perturbations do become greater as the levels of EV charging increase, no voltage violations occur. This further emphasizes that distribution bus voltages alone may not be an effective metric for determining grid health.

There are several other reasons distribution bus voltages may be an inadequate metric for determining relative grid health. First, in each case study, the buses that experienced the most voltage perturbations were near the end of the networks. Often utilities only take voltage measurements at the substation or select buses. Voltage is a local variable; it does not indicate the health of the grid at other locations within the same network. If grid health is evaluated based on voltage data taken at the substation, there may be voltage violations on remote buses due to EV charging which go unnoticed. Second, voltage perturbations on distribution networks are often masked by the operation of voltage regulators. If voltage regulators change tap positions to bring bus voltages back to nominal, bus voltages will not indicate the health of the grid. For the simulations in these case studies, the voltage regulators in the network models were disabled to avoid this masking effect, but it is unlikely any utilities would be willing to do so on a real system.

Some possible alternative metrics for grid health include line and transformer loading

and regulator action frequency. Heavily-loaded transformers and substation equipment will heat up, which drives the degradation of the equipment, accelerating the timeline to replace them before (or after) they fail. Load levels of this equipment, measured by field equipment or modeled in simulation, could serve as a second metric alongside bus voltages to characterize grid health. As mentioned previously, voltage perturbations are sometimes masked by load tap-changer regulators, which physically switch taps to keep the voltage within bounds. Frequent switching will wear out the unit faster, thus impacting grid health. Estimating the average switching frequency could serve as another useful grid health metric.

3.6.6 Outcomes

Section 3.6 explored the effectiveness of distribution bus voltages as a viable metric for grid health. Three case studies were performed using the Caldera software, which uses EVSE and distribution network models to develop time-series voltage data for various buses on the network. The IEEE 34-bus system model and a model of a distribution network in SLC were used in the three case studies. The simulation results show that while voltage violations occur on the IEEE 34-bus model, voltage violations do not occur on a model of a real distribution network despite the level of EV charging. This indicates distribution bus voltages alone may be a poor metric for grid health and that determining grid health is a complex problem that is beyond the scope of the research presented in this proposal. Consequently, the model presented in this proposal will rely on historical data for dynamic electricity prices.

CHAPTER 4

Algorithm Development

4.1 Objective Function

The cost of operating the microgrid model presented in Chapter 3 is simulated using linear programming optimization. Linear programming is a mature, well-documented optimization algorithm and is well-suited to the present application. The preeminent component of linear programming optimization is the objective function. The objective function defines what aspect of the optimization model is undergoing optimization. Each of the six simulations is optimized for cost. That is, the cost of operating the microgrid is minimized over 24 hours. The optimization is repeated for each day of the month as each day has different loading and solar output.

The objective function and the optimization algorithm change depending on what utility pricing structure is being simulated. The differences between the objective functions are highlighted and discussed in the following sections.

Because only the operation costs are considered in this research and capital costs are neglected, energy from the battery storage system and the PV array have no associated costs. The only way in which the microgrid induces expenses is through its interaction with the utility. The microgrid must purchase power from the utility if its own generation and/or storage cannot serve the instantaneous load. The microgrid may also use the utility power system to charge the battery storage in which case the battery storage acts as a load.

The equations developed in Chapter 3 to model the different technologies and functions of the microgrid serve as the constraints for the optimization problem. The decision variables are the times at which the battery storage system charges and discharges and the net power drawn from the grid. In each case study, the optimization minimizes the microgrid's operational cost by adjusting the battery storage dispatch schedule.

The objective function and the optimization algorithm change depending on what utility pricing structure is being simulated. The differences between the objective functions are highlighted and discussed in the following sections.

4.2 Algorithm Design

Each simulation covers one month of microgrid operation. The simulation is run for 31 iterations representing each day in July. Each iteration covers 24 time steps equal to 24 hours of operation. This models a microgrid operator having access to price estimates for the next 24 hours and scheduling the microgrid's resources accordingly. The simulation is then looped for each day of the month, and the net power of the battery storage system and the net grid power are recorded for each iteration. At the end of the simulation, the energy consumed and generated by the microgrid is known for every hour of the month. Figure 4.1 is a diagram showing the flow of the simulation algorithm.

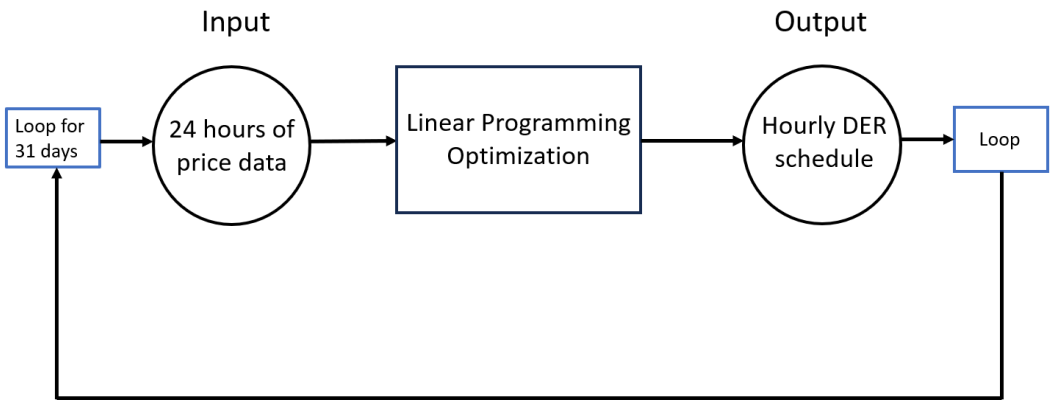

Fig. 4.1: Simulation flowchart.

4.2.1 Traditional Rate Schedule Simulation

For the first simulation, the model will use a traditional rate schedule and the price of electricity will be constant. This could model a seasonal price as the case studies only cover the month of July. The average cost of electricity in the US in July 2022 was $0.16

per kWh [55]. This price will be used in the first simulation.

The objective function for the first simulation is given by equation 4.1. The term inside the summation is the net power drawn from the grid at each hour multiplied by the price of electricity for the corresponding hour. As discussed, the price of electricity is a constant \$0.16 per kWh every hour for the first simulation. The result of the summation is the total cost of operation for the microgrid over 24 hours and is the variable optimized by the linear programming algorithm. Note for the first simulation, the demand charge is not included in the objective function but it is included in the total cost of operation reported in Chapter 5.

$$\min \left(\sum_{t}^{T} (\text{grid}(t) * \text{Price}(t)) \right) \tag{4.1}$$

4.2.2 Dynamic Price Simulation

As discussed in Chapter 3, the dynamic price model used for the simulations using dynamic pricing is constructed from historical electricity price data. The historical price data used in this research is for an area in Texas and was obtained from public records published by the Electric Reliability Council of Texas (ERCOT) [56]. The data set contains hourly prices for July 2022 and is shown in figure 4.2.

The raw data obtained from ERCOT is adjusted to be more compatible with the microgrid model and to be more suitable to the scope of the research. The data is scaled to result in a price per kWh instead of per MWh. Additionally, each data point in figure 4.2 is adjusted upwards by \$0.05 resulting in the average price over the month being \$0.16 per kWh. This is done to facilitate a more useful comparison to the results of the simulations using the traditional rate schedule. Figure 4.3 shows a graph of the adjusted price data.

The objective function for the second simulation is identical to equation 4.1. Except for the data set used for the hourly prices, all aspects of the algorithm and the software remain unchanged from the first case study. Again, demand charges are not included in the objective function but are included in the total cost of operation.

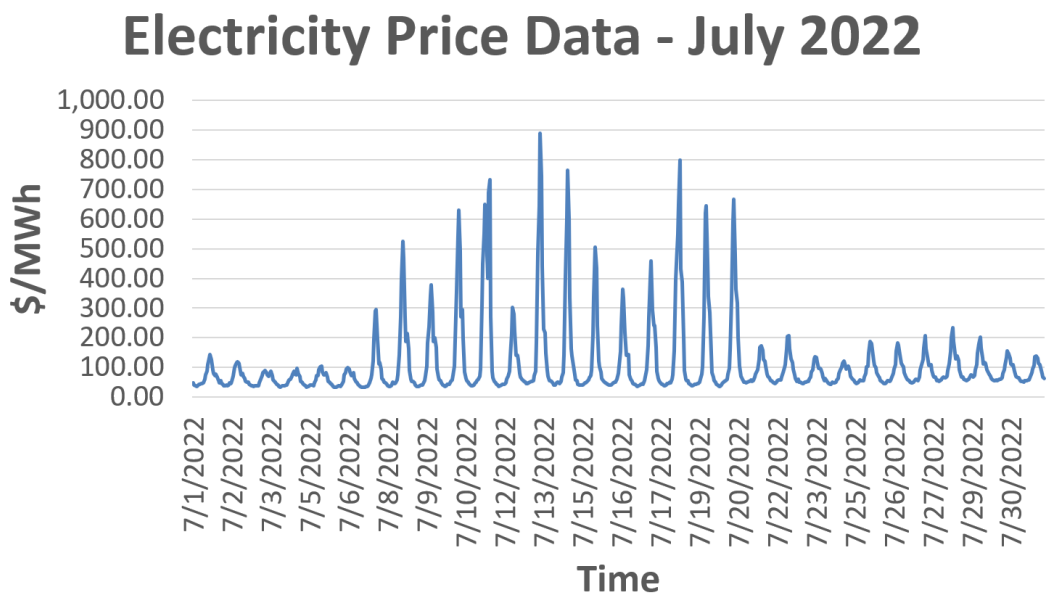

Fig. 4.2: Historical prices data set for July 2022.

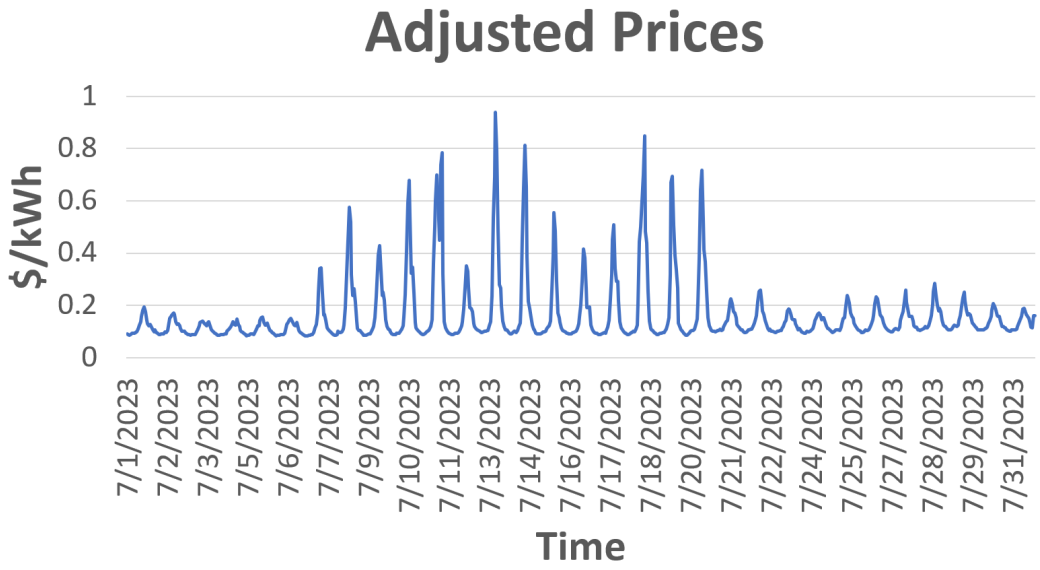

Fig. 4.3: Adjusted prices.

4.2.3 Dynamic Price and Demand Charge Simulation

In the third simulation, the demand charge is included in the objective function. Consequently, the optimization will make decisions to minimize both the total energy imported from the grid and the peak demand. Because each optimization interval is over 24 hours,

the controller minimizes the demand charge daily instead of monthly. At the end of the simulation, the daily demand charges are subtracted from the total operation cost, and the single peak monthly demand charge is added back to the total operation cost.

In software, the demand charge is simply the maximum hourly grid power for the day multiplied by the cost per kW. As stated previously, the cost per kW used is $10 per kW.

The objective function in the third simulation is modified to include the demand charge as shown in equation 4.2 where the demand charge is $10 per kW.

$$\min \left(\sum_{t}^{T} (\text{grid}(t) * \text{Price}(t)) + \max(\text{grid}(t)) * \text{demand} \right) \tag{4.2}$$

4.2.4 Microgrids with EV Charging

The final three simulations are identical to the first three simulations respectively except for the load model used. The load model used in the final three simulations includes EV charging as discussed in section 3.4.2. The EV charging load consists of two 100 kW EV charging sessions each day. Figure 3.4 shows the load profile used in the final three simulations

4.3 Software Implementation

Each simulation is implemented with the Python programming language following the flowchart shown in figure 4.1. The linear programming optimization algorithm will be implemented with a third-party library called docplex [57]. This library is part of IBM's CPLEX Python tools and will streamline the software structuring of the objective functions, constraint equations, and decision variables.

Figure 4.4 shows a flowchart of the high-level implementation of the algorithm in software. The implementation consists of two loops. The inner loop builds the optimization problem using the input data for the day by instantiating constraint equations for each hour of the day. Across 24 hours and all the constraints, there are 169 constraint equations in each optimization. At the end of the inner loop (once for each day), the objective function is applied and the linear programming problem is solved. The output of the solve function

is the optimal value for the decision variables. This is the optimal DER dispatch for the day. This data is then collected and the process is done for the next until each day of the month has been optimized. On an AMD 7700x processor, the full optimization for the month takes less than five seconds to solve.

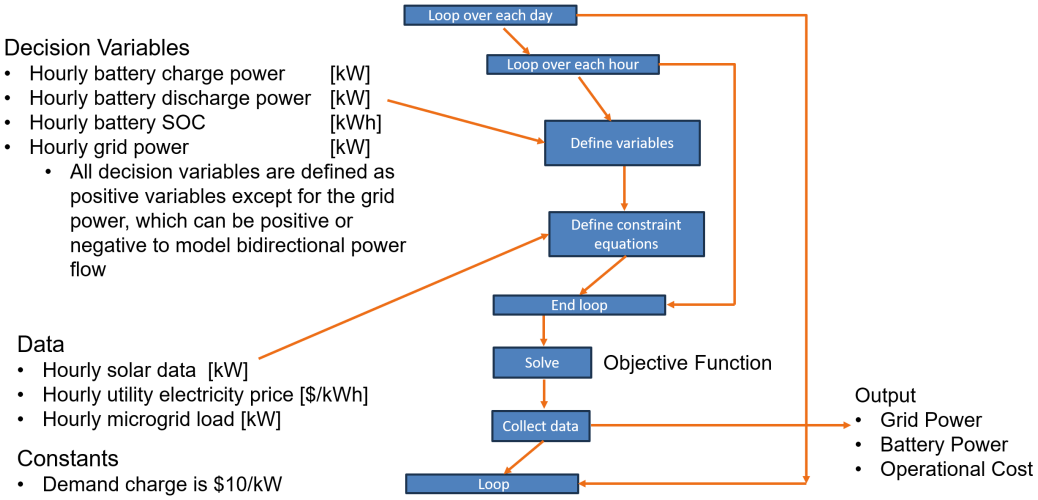

Fig. 4.4: Software flowchart.

CHAPTER 5

RESULTS AND ANALYSIS

The results of each case study include the total cost of operation over the month, the energy imported from and served to the grid, and the energy mix each hour of the month. Tables 5.1 and 5.2 tabulate the cost results of each simulation and the energy exchanged with the grid respectively.

Table 5.1: Cost results of the case studies.

	Sim 1	*Sim* 2	*Sim* 3	*Sim* 4	*Sim* 5	*Sim* 6
Energy Charge	\$10,486	\$7,525	\$8,258	\$11,478	\$8,710	\$9,880
Demand Charge	\$2,264	\$2,225	\$1,180	\$2,264	\$2,890	\$1,314
Total Cost	\$12,750	\$9,750	\$9,438	\$13,742	\$11,600	\$11,194

Table 5.2: Energy imported from and exported to the grid.

	Sim 1	*Sim* 2	*Sim* 3	*Sim* 4	*Sim* 5	*Sim* 6
Imported [kWh]	69,401	68,068	65,535	74,722	74,000	71,735
Exported [kWh]	3,866	2,533	0	2,987	2,264	0
Total Revenue	\$618.54	\$889	\$0	\$478	\$785	\$0

The results of the simulations also include graphs of the energy mixes serving the microgrid for each simulation. The following subsections detail the hourly energy mix for each simulation. Only a subset of the monthly data covering the same five days is shown in the following sections to facilitate analysis of the salient features of the results. For each energy mix, the sum of the instantaneous load, solar, grid, and battery is zero such that the load balance constraint is met. Note that a negative value for the battery power here indicates energy from the battery is leaving the microgrid and the microgrid's output exceeds its load. A positive value for the battery power corresponds to when the battery is charging and acting as a load. Similarly, a negative grid power indicates the microgrid is

contributing power to the grid. A positive grid power indicates the microgrid is consuming power from the grid.

Also shown in the following sections is the battery storage SOC over the same period graphed for the energy mix. These graphs give insight into the battery's operation for the rate structure and load model used for each simulation. The battery SOC is given at each hour over the graphed interval and is shown in kWh. Note that as prescribed by the battery model presented in Chapter 3, the battery SOC must remain between 400 kWh and 120 kWh and have a maximum capacity of 400 kWh.

The results and analysis of the simulations for each of the rate structures are presented below. For convenience, the analysis is broken into two parts: a discussion of the control implications drawn from the results and a discussion of the operational costs of each case study.

5.1 Traditional Rate Schedule

Figure 5.1 shows the energy mix resulting from the simulation using a traditional rate structure with a constant price signal of $0.16 per kWh. The left-hand vertical axis shows the power contributed by each source and the power of the load at each time step. Note that because the optimization is run with time steps of an hour, the data plotted against the left-hand vertical axis shows both the power at each hour and the energy contributed or consumed at each hour. The right-hand vertical axis shows the price of electricity per kWh at each time step. Figure 5.2 shows the battery SOC for this simulation.

Figure 5.3 shows the energy mix resulting from the simulation using a traditional rate schedule and a load model including EV charging. Figure 5.4 shows the battery SOC for this simulation.

5.1.1 Operations Analysis

The most visually obvious difference between the energy mixes from the simulations with a traditional rate schedule and those with a dynamic price signal is the high frequency with which the battery storage vacillates as seen in figures 5.1 and 5.3. Because the battery

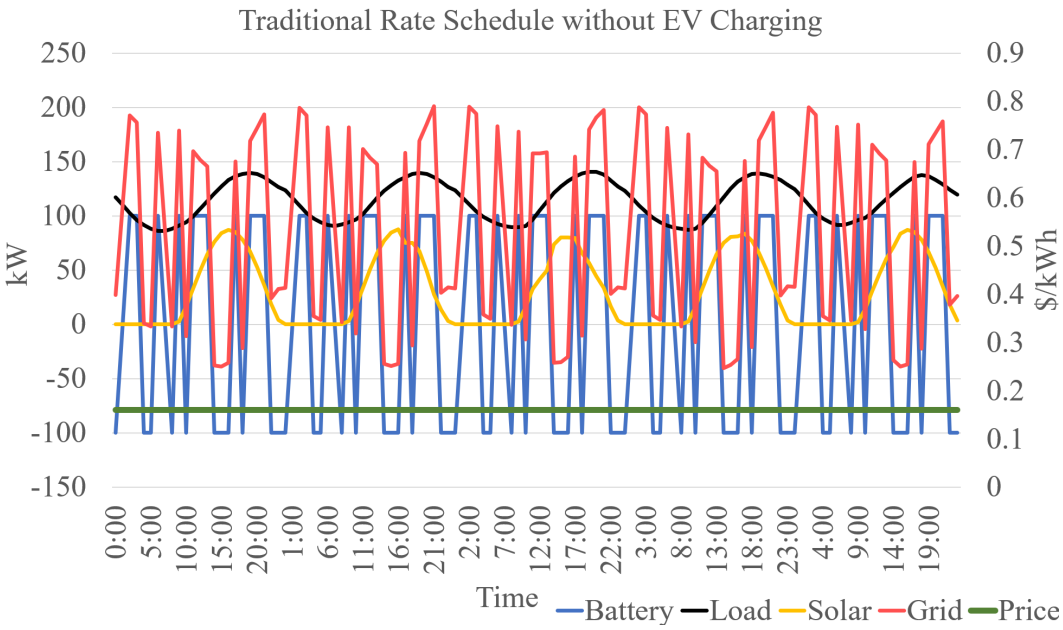

Fig. 5.1: Traditional rate structure simulation energy mix.

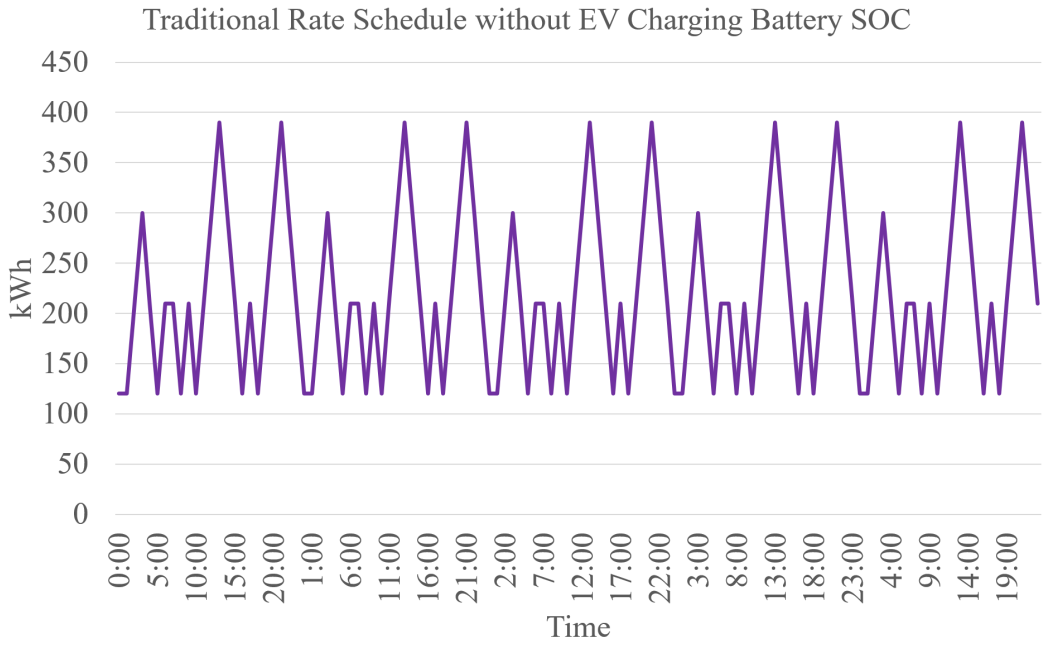

Fig. 5.2: Traditional rate schedule simulation battery SOC.

storage is highly variable in these simulations, the grid power is consequently highly variable as well to maintain the load balance constraint.

Because the price is constant, it does not matter when the battery charges or discharges.

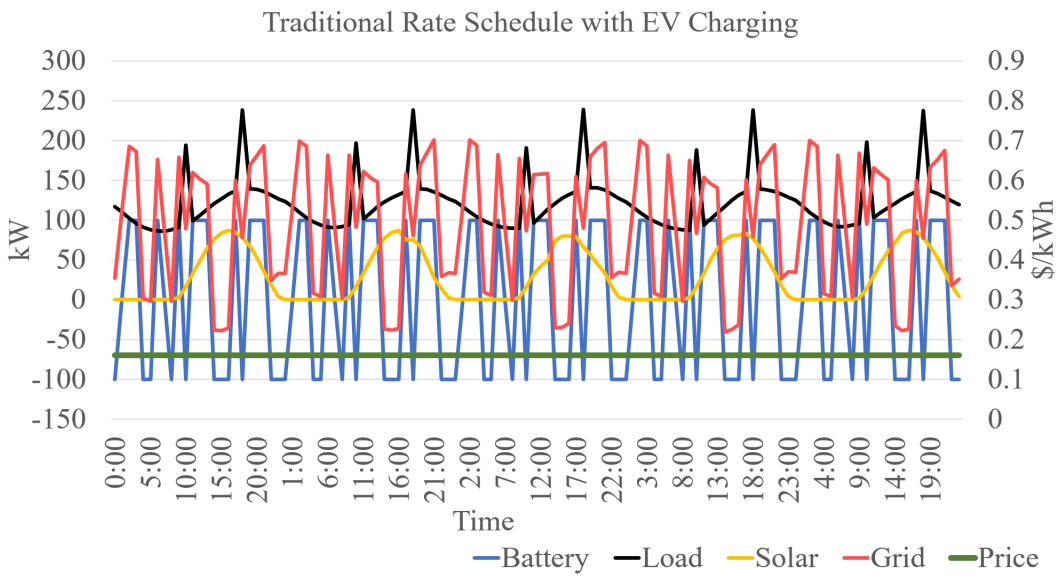

Fig. 5.3: Traditional rate schedule with EV charging energy mix.

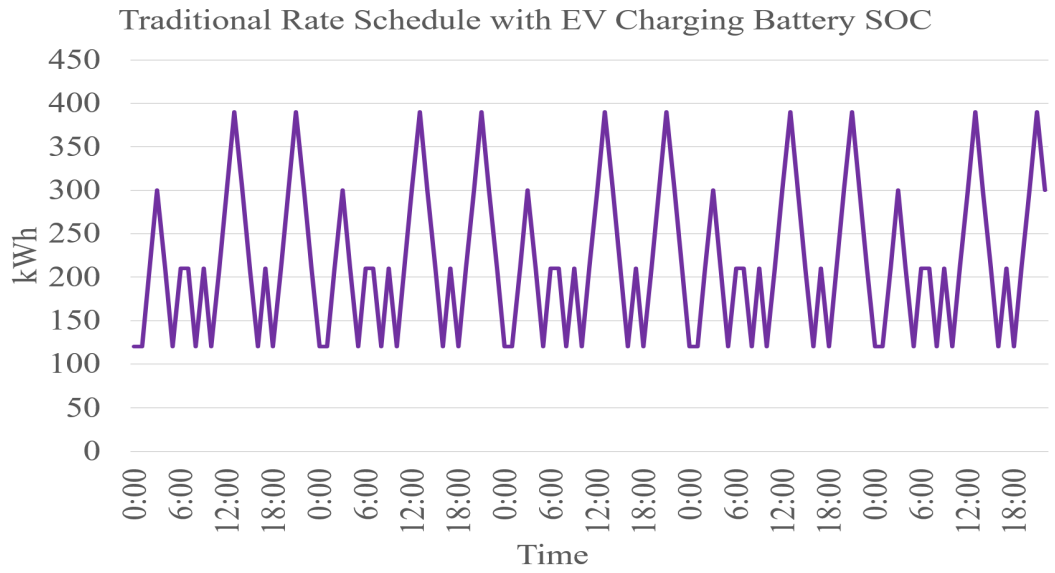

Fig. 5.4: Traditional rate schedule with EV charging battery SOC.

The cost of doing so is the same across all time steps, and because the algorithm optimizes for cost without regard to the demand charge, the battery charging and discharging times are irrelevant to the optimization. This fact manifests itself graphically in the highly variable battery and grid powers shown by the blue and red lines respectively in figures 5.1 and 5.3. For these algorithms, it is optimal to use the energy from the battery storage as much and

as quickly as possible.

In these simulations, the battery is operated frequently and aggressively. Over the period plotted, the battery is nearly always operating. It is also primarily operating at its maximum rate while both charging and discharging. While this is the optimal control strategy for a traditional rate schedule, operating battery storage systems in such a way degrades the battery's lifetime. Consequently, the algorithm could potentially result in higher capital costs in the long term if the battery storage system must be replaced sooner. Additionally, having such high variability in system power flows wears other components such as switches and sensing equipment. These optimization algorithms find the optimal control strategy when only operation costs are considered, but to find a more practical control strategy the model must be modified to include additional variables.

There is little operational difference between the simulations using a traditional rate schedule due to EV charging. This is because there is little to optimize in these cases. The price is constant and demand charges are not included. The periodic spikes in load caused by the EV charging does little to change the optimization.

5.1.2 Cost Analysis

The simulations using a traditional rate schedule act as a baseline for the other simulations. Because the electricity price is constant, the optimization algorithm results in relatively random behavior as can be seen in figures 5.1 and 5.3. The objective function minimizes the cost of operating the microgrid, and because the electricity price is constant, there is no benefit to charging and discharging the battery at specific times over others. Figures 5.2 and 5.4 show that the energy in the battery is used as soon as the battery reaches its maximum SOC. The electricity price drives the choices made by the optimizer. Because the price is constant, there is no control choice that is more optimal than another.

Table 5.2 shows for these simulations there were instances when energy was pushed back to the grid from the microgrid, which resulted in revenue for the microgrid. However, when the electricity price is constant, there is little incentive to do this because power is purchased and sold at the same rate. If energy is imported from the grid, stored in the

battery for a time, and then sold back to the utility, no profit is made and there is no benefit. There is some loss in this scenario due to the inefficiencies of the battery and the inverter. The only scenario in which this is a profitable control strategy given a traditional rate schedule is when the solar produces more energy than is needed by the microgrid's load. However, as can be seen in figures 5.1 and 5.3, there is no instance when the solar output is higher than the load. The controller pushing energy back to the grid in these simulations is largely due to the random control behavior caused by the constant price.

5.2 Dynamic Pricing

Figure 5.5 shows the energy mix from the simulation with a normal load model and dynamic prices with an average price of $0.16 per kWh and no demand charge. Figure 5.6 shows the battery SOC for this simulation.

5.2.1 Operations Analysis

The simulations using a dynamic price result in a lower frequency battery charging and discharging pattern relative to traditional rate schedule simulations. The battery charging and discharging pattern follows a diurnal cycle in the cases using a dynamic price signal. This is caused by the diurnal pattern in the dynamic price signal shown in figure 4.3. The green line superimposed on the energy mix in figures 5.1 - 5.11 shows the price signal at the same time steps as the energy mix. The dynamic price signal, shown in figure 4.3, spikes in the early evening, which is typical of most commercial and residential load patterns.

Figure 5.7 shows the energy mix resulting from the simulation using a dynamic price and a load model including EV charging. Figure 5.8 shows the battery SOC for this simulation.

The battery is charged daily in the early morning when the price is lowest. During this time, the controller draws energy from the grid at the maximum rate to charge the battery quickly before the price increases again. The algorithm maximizes the energy outputted from and inputted to the battery during the most optimal charging and discharging times by nearly always operating the battery at its maximum rate as seen in figures 5.5 and 5.7.

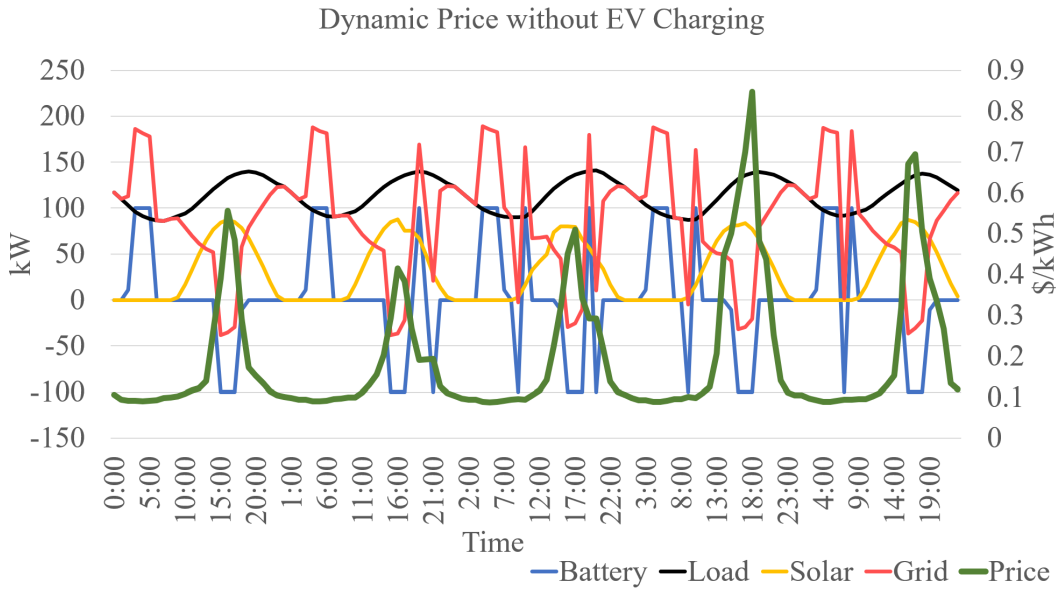

Fig. 5.5: Dynamic price with a normal load model simulation energy mix.

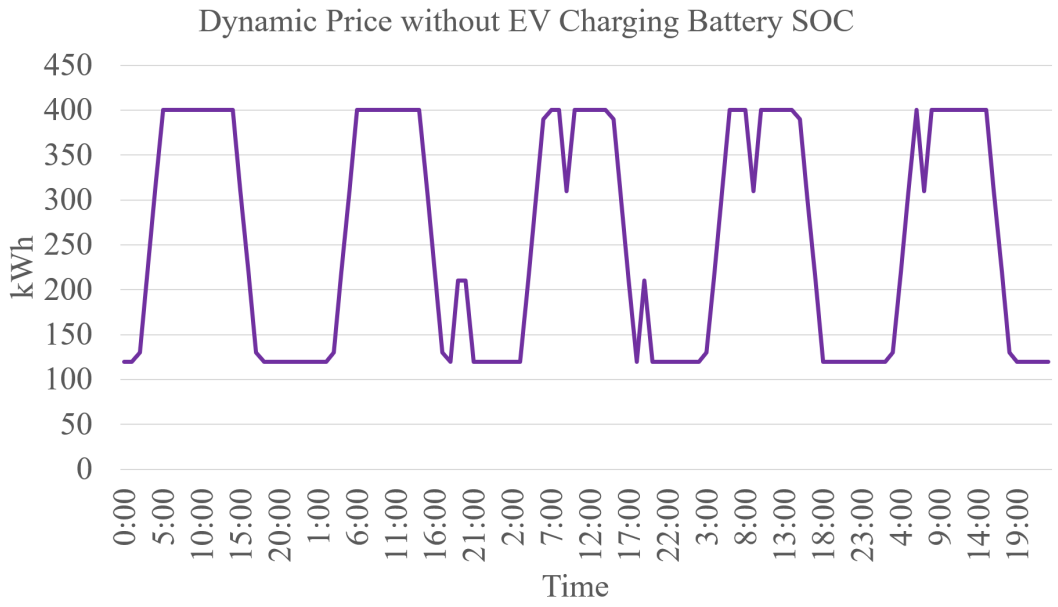

Fig. 5.6: Dynamic price with a normal load model battery SOC.

Essentially, the control system keeps the battery energy in reserve until the most optimal moment to discharge, which corresponds to when the price is highest. As seen in figures 5.5 and 5.7, this results in significant downtime for the battery compared to the traditional rate schedule simulations. In the simulations using a dynamic price, the battery is idle for

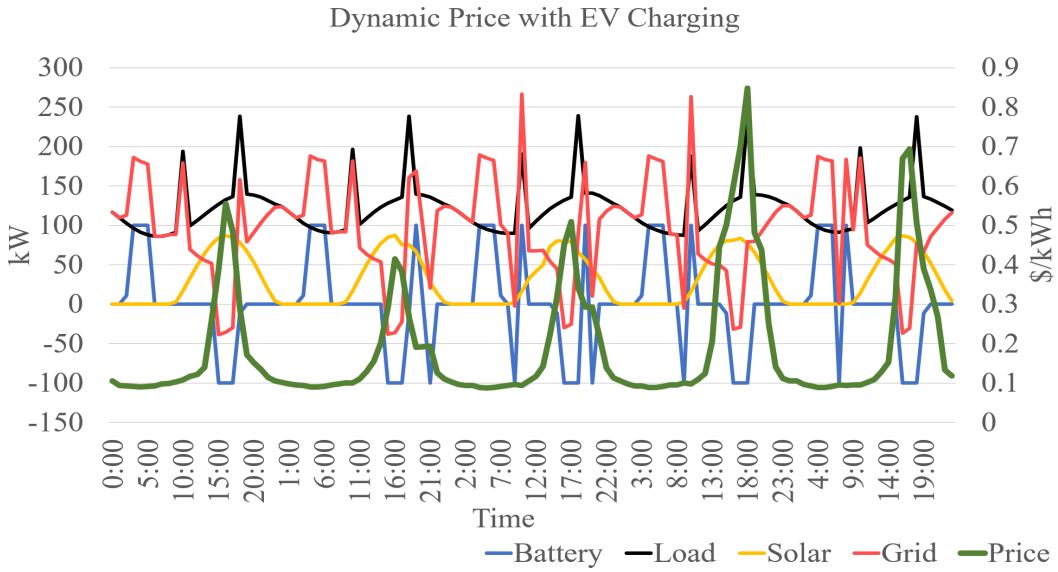

Fig. 5.7: Dynamic price with a load model including EV charging simulation energy mix.

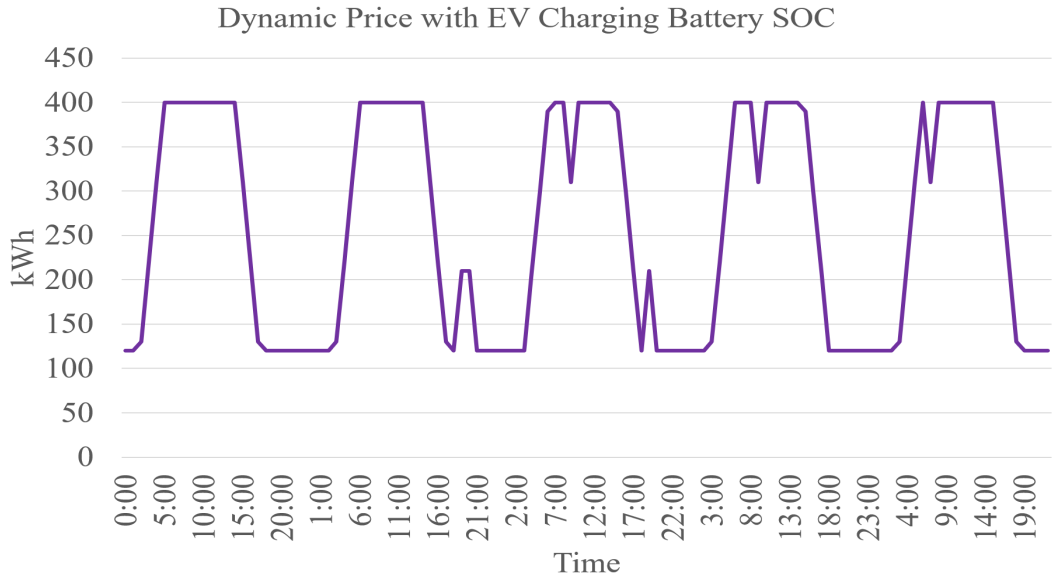

Fig. 5.8: Dynamic price with a load model including EV charging simulation battery SOC.

substantial portions of the day. In contrast to the traditional rate schedule simulations, it is no longer irrelevant when the battery charges and discharges. The dynamic price signal causes the algorithm to dispatch the battery at specific times namely when the price is highest and the cost of importing energy from the grid is the highest.

While it is generally true that the optimizer charges the battery when the price is

the lowest, there are exceptions. It can be seen in figures 5.5 and 5.7 that there are brief periods where the controller charges the battery at times when the price is highest. This seemingly less-than-optimal behavior is explained by comparing the plot of the battery power to the corresponding plot of the battery's SOC. Figures 5.6 and 5.8 show that when the battery charges during times when the price of electricity is high, the battery SOC is at its minimum. The control attempts to fill the battery as much as possible just before the price of electricity is at its true maximum.

Introducing EV charging to the dynamic price model does not significantly change the control optimization as seen by comparing figures 5.5 and 5.7. The most notable change in the energy mix is the load spikes corresponding to the EV charging sessions. These load spikes unsurprisingly result in corresponding spikes in power consumed by the grid when there is EV charging. However, Table 5.2 indicates that less energy is imported from the grid in the dynamic price simulations compared to the traditional rate schedule simulations. This is the result of the algorithm optimizing when the battery charges and discharges to minimize energy imports. Less energy from the battery is used to serve the microgrid's load in cases with dynamic charging.

5.2.2 Cost Analysis

The optimal control behavior in the dynamic price simulations as seen in figures 5.5 and 5.7 is notably more deterministic than in traditional rate schedule simulations. Now that the electricity price is dynamic, the optimizer has an incentive to dispatch the battery at certain times over others. The optimal behavior primarily discharges the battery during times of high price and charges during times of low price. Drawing power from the grid during traditional peak loading times, which occurs during the early evening hours, is far more costly than if the same amount of energy was used during off-peak times. Figures 5.6 and 5.8 show that after the battery is charged to its maximum capacity, it is idle for a period before it is discharged. The optimizer saves the less expensive energy in the battery for use during times when the electricity price is high.

Table 5.2 indicates that the dynamic price simulations imported less energy from the

grid than the traditional rate schedule simulations. In the traditional rate schedule simulations, the battery was charged as frequently as possible. Energy was not held in reserve. There was no time when the battery was idle. Consequently, more energy overall was used from the grid to charge the battery. The dynamic price simulations have times when the battery is idle, which can be seen in both the SOC figures when the energy in the battery is constant and in the energy mix figures when the battery power is zero. Throughout the optimization, this behavior results in less power being imported from the grid and a reduced energy cost as seen in Table 5.1.

Table 5.2 also shows that the dynamic price simulations result in less energy exported to the grid than the constant price cases. However, table 5.2 also shows that despite exporting less energy, the dynamic price cases resulted in higher revenue. Figures 5.5 and 5.7 show that when the controller exports power to the utility (when the grid power is negative), the electricity price is also at its daily peak. The price differential between when the controller exports power in the traditional rate schedule simulations and the dynamic price simulations allows the dynamic price simulations to have greater revenue despite exporting less energy. The optimization in the dynamic price simulations results in arbitrage behavior where energy is purchased from the grid when the price is low and then sold back to the grid when the price is higher. Arbitrage, along with less imported energy, results in a lower overall operation cost in the dynamic price simulations as shown in table 5.1.

5.3 Dynamic Prices and Demand Charge

Figure 5.9 shows the energy mix resulting from the simulation using a normal load model and a dynamic price including a demand charge of $10 per kW. Figure 5.10 shows the battery SOC for this simulation.

Figure 5.11 shows the energy mix resulting from the simulation using a dynamic price and demand charge and a load model including EV charging. Figure 5.12 shows the battery SOC for this simulation.

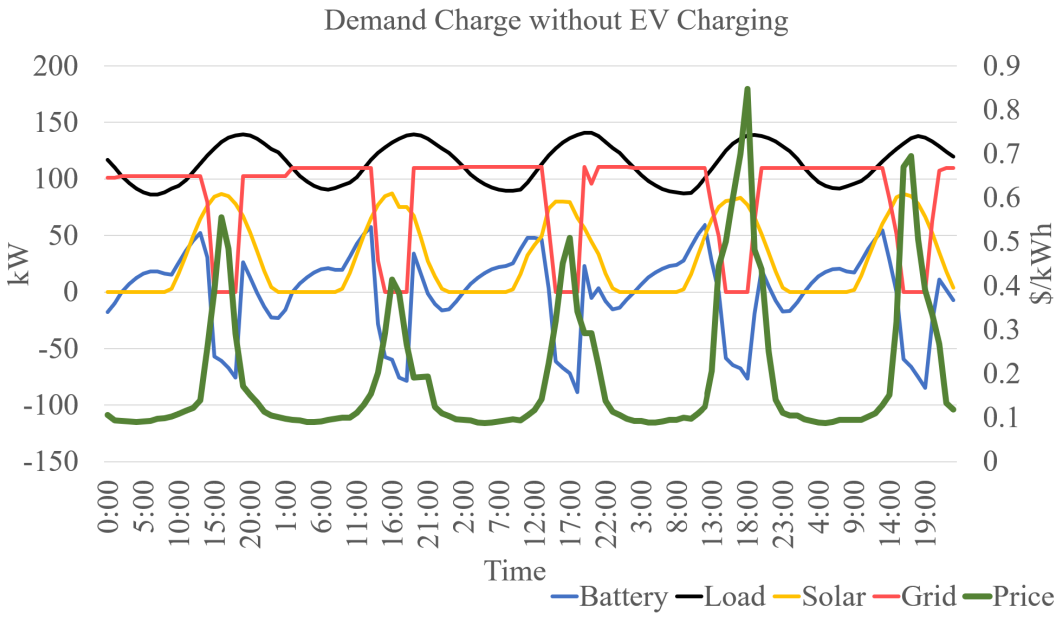

Fig. 5.9: Dynamic price including demand charge with a normal load model simulation energy mix.

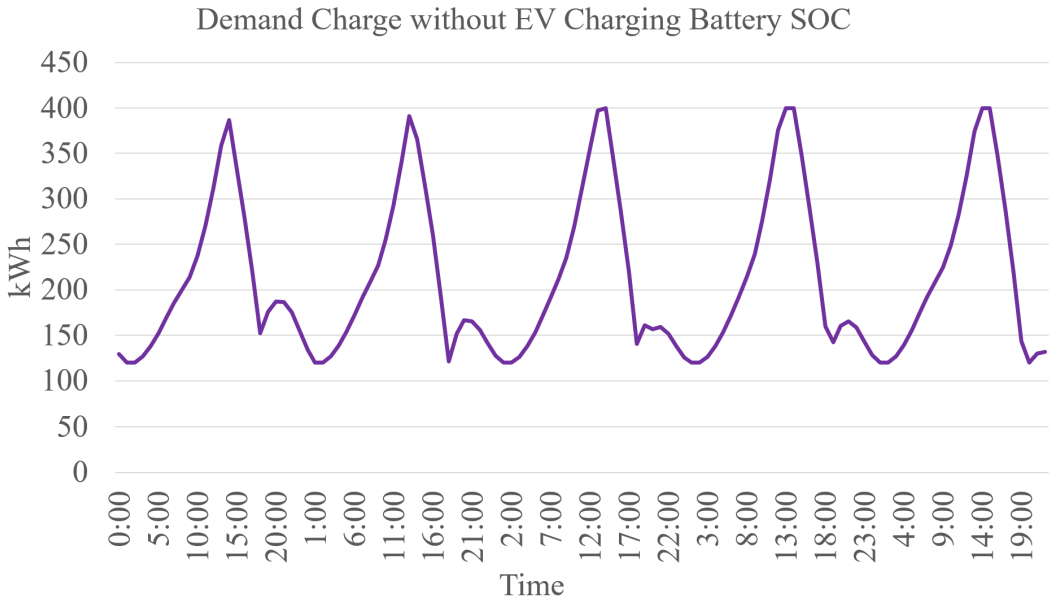

Fig. 5.10: Dynamic price including demand charge with a normal load model simulation battery SOC.

5.3.1 Operations Analysis

Including the demand charge in the objective function significantly changes the form of the energy mix graphs. The most salient change between figures 5.9 and 5.11 and the

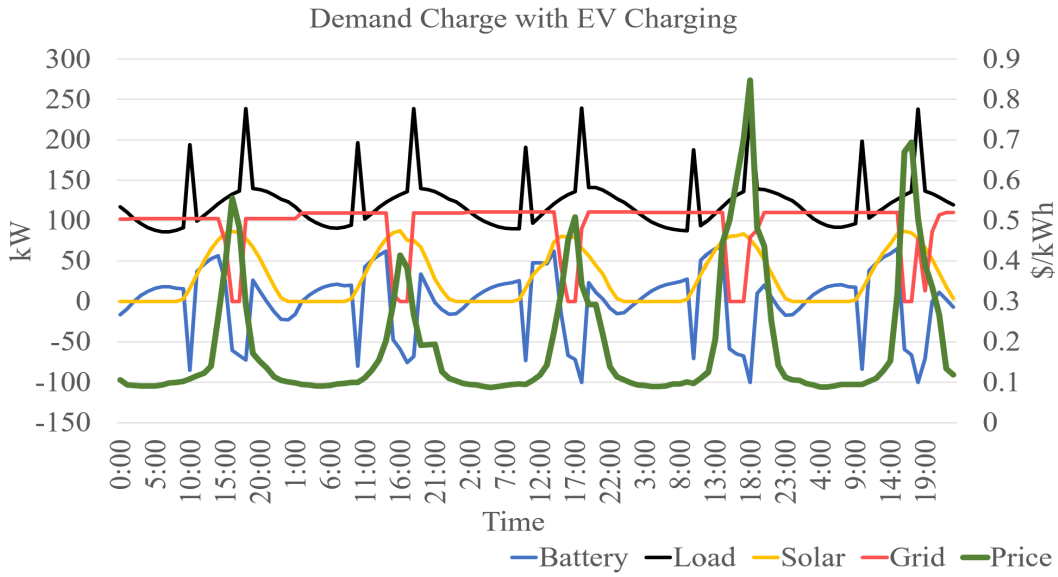

Fig. 5.11: Dynamic price including demand charge with a load model including EV charging simulation energy mix.

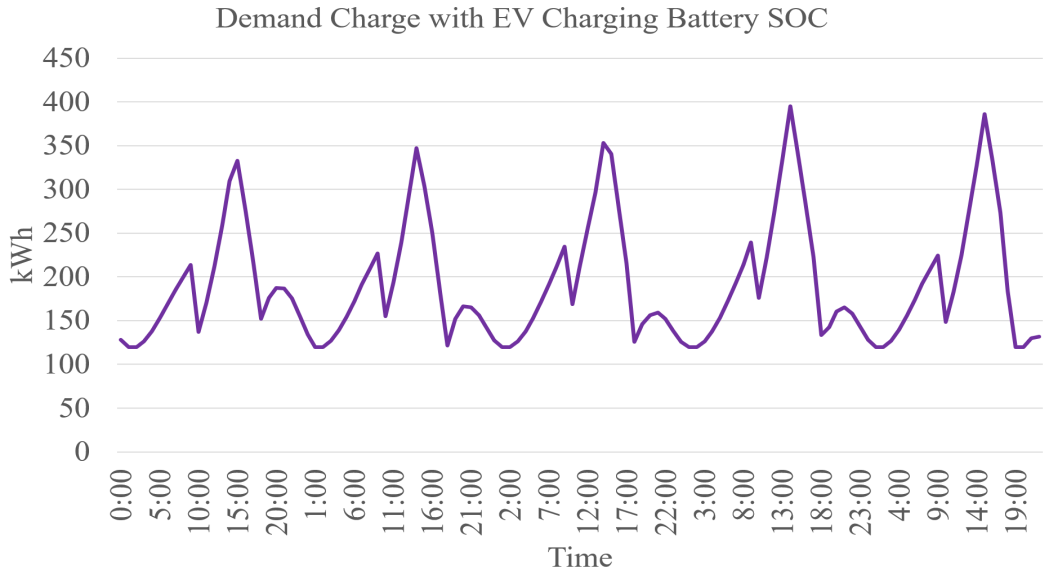

Fig. 5.12: Dynamic price including demand charge with a load model including EV charging simulation battery SOC.

energy mix charts from the simulations which do not include demand charges in the objective function is the nearly constant grid power. As the daily peak grid power increases, so does the monthly demand charge. Consequently, the controller holds the power imported from the grid constant at the value needed to cover the microgrid's daily load. This behavior

would be marginally different if the optimization period were the full month. Each time during the month when the imported grid power necessarily peaked due to low solar output or unusually high loads, that peak power would become the new maximum power the microgrid could draw from the grid without incurring additional demand charges. For the implementation of the optimization algorithm in demand charge simulations, this process takes place over a day instead of a month.

In the simulations where demand charge is not part of the objective function, periodic spikes occur in the grid power. These spikes correspond to either battery charging, EV charging, or both. When demand charges are included in the optimization, the controller changes the battery charging behavior seen in the previous simulations. Previously, the controller would wait for the lowest price and charge the battery as quickly as possible during that time, which would result in a spike in grid power. The controller would then keep this energy in reserve until the most optimal time to discharge, which typically corresponded with the highest price.

In the demand charge simulations, the battery is charged more gradually over a longer period when the electricity price is low as seen in figures 5.9 and 5.11. This energy is then used as soon as the battery reaches maximum SOC as seen in figures 5.10 and 5.12. Similar to the charging pattern resulting from dynamic price optimization, the battery in the demand charge simulations discharges quickly once it is filled. This is done to offset the peak load and to avoid paying the peak electricity price. When the battery discharges, the grid power falls to zero. This is the time of peak solar output, which also contributes to preventing high grid power peaks. Because the controller uses all available energy to keep grid power peaks as low as possible, no power is exported to the grid in the demand charge simulations. As seen in figures 5.9 and 5.11, the grid power never goes below zero.

Despite more consistently using grid power in the demand charge simulations, table 5.2 shows that less energy is imported from the grid overall when demand charges are included in the optimization even when EV charging is included in the microgrid load. Figures 5.10 and 5.12 support this conclusion by showing the average SOC of the battery is lower

than in the simulations where demand charges are not included in the objective function. Less energy is stored in the battery throughout the optimization, and because a significant portion of the energy used to charge the battery comes from the grid, less energy is imported from the grid.

5.3.2 Cost Analysis

Figures 5.5 and 5.7 show that in the dynamic price simulations, the battery is charged over as short of a period as possible, which results in a high charging power and a high demand on the grid. Including demand charge in the objective function has the effect of removing the spikes in grid power caused by charging the battery quickly. Lowering the peak grid demand lowers the demand charge as well. Table 5.1 shows that in the demand charge simulations, the demand charge was over $1,000 less than the simulations where the demand charge was not included in the objective function.

The demand charge simulations resulted in less energy imported from the grid than the simulations where the demand charge was not included in the objective function. Table 5.2 shows that demand charge simulations imported nearly 3,000 fewer kWh of energy from the grid than the demand charge simulations. However, table 5.1 shows that the energy charge increased significantly when the demand charge was included in the objective function compared to the dynamic price simulations. The demand charge simulations import energy from the grid more consistently than the other cases as indicated by the nearly flat line for grid power in figures 5.9 and 5.11. While less energy is imported from the grid overall in the demand charge simulations, more energy is imported during times when the electricity price is high than in the dynamic price simulations where the grid power is kept low when the price is high. This causes the energy charge to increase while the actual kilowatt hours of energy imported decreases.

In the demand charge simulations, the controller must find the optimal balance between demand charges and energy charges. Table 5.1 shows that the optimal balance for the microgrid and scenario modeled here results in a total cost that is slightly lower than the dynamic price simulations. For the microgrid modeled in this research, including demand

charge in the objective function resulted in both lower operational costs and lower energy imported from the grid. However, it is not guaranteed that this is the case in general. Whether including demand charge in the objective function results in a more economical control strategy is highly dependent on the combination of DERs connected to the microgrid, the microgrid's load, and the policies of the local utility. If the balance between using the battery for arbitrage and using it to reduce peak demand changes, a different algorithm may result in more cost savings.

The effect of EV charging is more clearly seen in the demand charge simulations. Comparing the dynamic price simulation without EV charging to the dynamic price simulation with EV charging reveals that the peak grid power is significantly higher when EV charging is present on the grid as seen by comparing figures 5.5 and 5.7. However, the grid power is nearly the same as the demand charge simulations, which implies including demand charge in the objective function reduced the peak demand more when EV charging was present. Table 5.1 shows that the demand charge was reduced by \$1,045. When EV charging is present on the microgrid, table 5.1 shows the demand charge was reduced by \$1,576 from the demand charge simulation without EV charging to the demand charge simulation with EV charging. The savings from demand charge reduction is greater when EV charging is present even when the increased imported energy is considered.

CHAPTER 6

CONCLUSION

Microgrids have already and will continue to play a significant role in the world's energy revolution and climate crisis. The research presented in this thesis develops methods for controlling microgrid DERs such that operating costs are reduced and microgrids become more economically available to a wider consumer base. This research contributes to this end and the existing body of research in the following ways:

1. Presents a distribution grid loading model.
2. Evaluates a method for determining grid health.
3. Develops an algorithm for cost-optimal microgrid control.
4. Implements the optimization algorithm in software.
5. Validates the optimization software.

The primary focus of the research is optimal control of microgrids when connected to utilities with various rate schedules and price structures particularly when the utility electricity price is dynamic. A major consideration in this research is how to accurately model dynamic utility prices. A method of creating a dynamic price model by determining local grid health was proposed and presented in chapter three. A distribution grid model was developed and simulated with various loads. Local bus voltages were used as a metric for determining the grid health and to serve as a basis for the dynamic price model. The results of the simulations indicated that distribution bus voltages alone may not be sufficient to accurately determine grid health and are consequently unsuitable to serve as a basis for a dynamic pricing model. This conclusion led to the decision to use historical data as the dynamic price model for the microgrid model.

A generic microgrid model consisting of solar, battery storage, and a connection to the utility was modeled mathematically and serves as the basis for an algorithm that finds the cost-optimal control strategy of the microgrid's resources. The optimization is cast as a linear programming problem with the operation cost as the objective function. Six cases were simulated using a combination of one of the pricing structures modeled (traditional rate schedule, dynamic prices, and dynamic prices with demand charges) with either a normal load model or a normal load model augmented with EV charging. Each simulation was implemented in software using the Python programming language and the CPLEX library.

The results of the optimizations show that in each simulation the optimized control algorithm reduced the cost of operating the microgrid. The cost savings were a combination of reducing energy imported from the grid, energy arbitrage opportunities, and demand charge reduction. Comparing the six simulations leads to the conclusion that while the optimization results in cost savings generally, its effectiveness in specific cases is highly dependent on the location of the microgrid, the policies of the local utility, and the microgrid's load. The more predictable the microgrid's load the more effective an optimized control strategy will be at reducing costs. To get the best results, the operators of the microgrid should tailor the optimization to fit local conditions.

REFERENCES

[1] A. Kahan, "Eia projects nearly 50% increase in world energy usage by 2050, led by growth in asia," Sep 2019. [Online]. Available: https://www.eia.gov/todayinenergy/detail.php?id=41433

[2] "World energy balances: Overview." [Online]. Available: https://www.iea.org/reports/world-energy-balances-overview/world

[3] O. Apata, A. V. Adebayo, and P. K. Ainah, "Renewable energy systems and the fourth industrial revolution," in *2021 IEEE PES/IAS PowerAfrica*, 2021, pp. 1–5.

[4] "Documenting a decade of cost declines for pv systems," Feb 2021. [Online]. Available: https://www.nrel.gov/news/program/2021/documenting-a-decade-of-cost-declines-for-pv-systems.html

[5] "Electricity per kwh in u.s. city average, average price, not seasonally adjusted," May 2023. [Online]. Available: https://data.bls.gov/pdq/SurveyOutputServlet

[6] K. Prabakar, "Microgrids." [Online]. Available: https://www.nrel.gov/grid/microgrids.html

[7] C. Sulzberger, "Pearl street in miniature models of electric generating station," April 2013. [Online]. Available: https://magazine.ieee-pes.org/marchapril-2013/history-7/

[8] J. S, "How electricity grew up? a brief history of the electrical grid...," Oct 2012. [Online]. Available: https://power2switch.com/blog/how-electricity-grew-up-a-brief-history-of-the-electrical-grid/index.html

[9] J. Maxwell, "A dynamical theory of the electromagnetic field," 1873.

[10] M. Whelan, S. Rockwell, and S. Normandin, "The history of the transformer," 2014. [Online]. Available: https://edisontechcenter.org/Transformers.html

[11] S. Groat, "Places of invention: A spark in the berkshires." [Online]. Available: https://berkshiremuseum.org/blog/places-invention-spark-berkshires/

[12] M. Guarnieri, "Who invented the transformer? [historical]," *IEEE Industrial Electronics Magazine*, vol. 7, no. 4, pp. 56–59, 2013.

[13] S. Patel, A. Larson, and A. Harvey, "History of power: The evolution of the electric generation industry," October 2017. [Online]. Available: https://www.powermag.com/history-of-power-the-evolution-of-the-electric-generation-industry/

[14] C. Marcy, "Eia study examines the role of high-voltage power lines in integrating renewables," June 2018. [Online]. Available: https://www.eia.gov/todayinenergy/detail.php?id=36393

[15] E. Csanyi, "The structure of electrical power systems (generation, distribution, and transmission of energy)," October 2017. [Online]. Available: https://electrical-engineering-portal.com/electric-power-systems

[16] B. Kergin, "Photo: Check out what vancouver's power lines used to look like," 2022. [Online]. Available: https://www.vancouverisawesome.com/history/photo-check-out-what-vancouvers-power-lines-used-to-look-like-5398322

[17] "Emergence of electrical utilities in america." [Online]. Available: https://americanhistory.si.edu/powering/past/h1main.htm

[18] "The history and evolution of the u.s. electricity industry." [Online]. Available: https://energy.utexas.edu/sites/default/files/UTAustin_FCe_History_2016.pdf

[19] "The progressive era key facts." [Online]. Available: https://www.britannica.com/summary/The-Progressive-Era-Key-Facts

[20] "A brief history of the electric utility industry."

[21] U.S. Congress, "Public Utility Regulatory Policies Act," 1978, 42 U.S.C. § 6941 et seq. [Online]. Available: https://www.govinfo.gov/content/pkg/STATUTE-92/pdf/STATUTE-92-Pg3160.pdf

[22] Smithsonian, "The public utility regulatory policies act." [Online]. Available: https://americanhistory.si.edu/powering/past/history4.htm

[23] F. E. R. Commission, "Electric power markets," May 2023. [Online]. Available: https://www.ferc.gov/electric-power-markets

[24] H. S. Parmesano and C. S. Martin, "The evolution in u.s. electric utility rate design," *Annual Reviews*, vol. Volume, pp. 45–94, 1983.

[25] Direct Industry, "Diesel gnerator set gf series," Online, accessed: June 3, 2023. [Online]. Available: https://www.directindustry.com/prod/fujian-yanan-power-group/product-103705-1030215.html

[26] o. energy and gas magazine, "Opra turbines," Online, accessed: June 3, 2023. [Online]. Available: https://energy-oil-gas.com/news/opra-turbines-2/

[27] E. Wood, "How gas turbine microgrids create smart megawatts," February 2017. [Online]. Available: https://www.govinfo.gov/content/pkg/STATUTE-92/pdf/STATUTE-92-Pg3160.pdf

[28] J. Hamilton-Antonson, "Benefits of a synchronous generator in a microgrid," September 2022, aCCESSED: June 12, 2023. [Online]. Available: https://www.powermag.com/benefits-of-a-synchronous-generator-in-a-microgrid/

[29] "Solar module," May 2018, accessed: June 12, 2023. [Online]. Available: https://www.sunrun.com/go-solar-center/solar-terms/definition/solar-module

[30] T. Hutchins, V. Linga, and A. Mey, "U.s. large-scale battery storage capacity up 35% in 2020, rapid growth set to continue."

[31] E. Bellini, "Lithium-ion storage is here to stay," May 2020, accessed: June 13, 2023. [Online]. Available: https://www.pv-magazine.com/2020/05/08/lithium-ion-storage-is-here-to-stay/

[32] M. M. Islam, M. Nagrial, J. Rizk, and A. Hellany, "General aspects, islanding detection, and energy management in microgrids: A review," *Sustainability*, vol. 13, no. 16, 2021. [Online]. Available: https://www.mdpi.com/2071-1050/13/16/9301

[33] A. F. Bastos and R. D. Trevizan, "Feasibility of 100% renewable-energy-powered microgrids serving remote communities," in *2023 IEEE Power Energy Society Innovative Smart Grid Technologies Conference (ISGT)*, 2023, pp. 1–5.

[34] M. K. Sharma, P. Kumar, and V. Kumar, "Intentional islanding of microgrid," in *2017 6th International Conference on Computer Applications In Electrical Engineering-Recent Advances (CERA)*, 2017, pp. 247–251.

[35] Y. You, G. Wang, C.-h. Zhang, and J.-r. Lian, "An improved frequency control method for microgrid in islanded operation," in *2013 2nd International Symposium on Instrumentation and Measurement, Sensor Network and Automation (IMSNA)*, 2013, pp. 296–299.

[36] Y. Ouyang and Y. Zou, "Static stability analysis of outer-loop control in grid-connected inverters under weak grid condition," in *2018 International Conference on Power System Technology (POWERCON)*, 2018, pp. 1472–1476.

[37] Y. Zhang, H. Liu, P. Song, and L. Wu, "Small-signal stability analysis of multiple grid-connected virtual synchronous generators," in *2018 China International Conference on Electricity Distribution (CICED)*, 2018, pp. 2034–2038.

[38] H. Nezamabadi and V. Vahidinasab, "Arbitrage strategy of renewable-based microgrids via peer-to-peer energy-trading," *IEEE Transactions on Sustainable Energy*, vol. 12, no. 2, pp. 1372–1382, 2021.

[39] A. Kadri and K. Raahemifar, "Is economic feasibility of bess energy price arbitrage jurisdiction dependent," in *2018 IEEE 61st International Midwest Symposium on Circuits and Systems (MWSCAS)*, 2018, pp. 1–4.

[40] E. P. Delos Reyes, R. A. Aguirre, G. Y. R. Garcia, and K. J. R. Rosano, "Sizing of battery energy storage system in a photovoltaic off-grid dc microgrid incorporating a lithium-ion linear degradation model," in *2022 IEEE PES 14th Asia-Pacific Power and Energy Engineering Conference (APPEEC)*, 2022, pp. 1–6.

[41] E. Knöchelmann, S. Tappe, T. Ortmaier, and A. Männel, "Cost-optimized control of dc microgrids based on characteristic diagrams," in *2019 IEEE International Conference on Industrial Technology (ICIT)*, 2019, pp. 1685–1691.

[42] Y. Huang, Q. Zhang, and M. Kang, "Energy scheduling framework of micro-grids considering battery lifetime," *IEEE Access*, vol. 10, pp. 25 016–25 024, 2022.

[43] P. Gupta, M. Ansari, and I. Ali, "Design and cost analysis of grid connected hybrid microgrid system," in *2021 IEEE 8th Uttar Pradesh Section International Conference on Electrical, Electronics and Computer Engineering (UPCON)*, 2021, pp. 1–6.

[44] E. Knöchelmann, A. Männel, B. Goetjes, S. Tappe, and T. Ortmaier, "Decentralized cost-optimized fuzzy control of dc microgrids," in *2019 IEEE Third International Conference on DC Microgrids (ICDCM)*, 2019, pp. 1–7.

[45] X. Li and R. Xia, "A dynamic multi-constraints handling strategy for multi-objective energy management of microgrid based on moea," *IEEE Access*, vol. 7, pp. 138 732–138 744, 2019.

[46] A. J. Headley, B. L. Schenkman, and D. M. Rosewater, "Discrete logic vs optimized dispatch for energy storage in a microgrid," in *2020 IEEE Power Energy Society General Meeting (PESGM)*, 2020, pp. 1–5.

[47] Y. Zhu, Q. Zhang, K. Liu, M. Han, Q. Chen, and Y. Liu, "Optimized capacity configuration of photovoltaic generation and energy storage for residential microgrid," in *2019 IEEE Innovative Smart Grid Technologies - Asia (ISGT Asia)*, 2019, pp. 1751–1755.

[48] R. Bhuvaneswari, S. Srivastava, C. Edrington, D. Cartes, and S. Subramanian, "Intelligent agent based auction by economic generation scheduling for microgrid operation," in *2010 Innovative Smart Grid Technologies (ISGT)*, 2010, pp. 1–6.

[49] National Renewable Energy Laboratory, "National solar radiation database," https://nsrdb.nrel.gov/, 2016, accessed on: 23-06-2023.

[50] University of Colorado Boulder, Department of Electrical Engineering, "Microgrid loading dataset."

[51] D. Energy. (2023) Energy demand charges explained: What they are and why you should care. Online. [Online]. Available: https://sustainablesolutions.duke-energy.com/resources/energy-demand-charges-explained/

[52] L. Miller, J. Morgan, R. Zane, and H. Wang, "Distribution bus voltages as a metric for grid health considering widespread public ev charging," 2023, pp. 1–6.

[53] K. P. Schneider and et al., "Analytic considerations and design basis for the ieee distribution test feeders," *IEEE Trans. Power Syst.*, vol. 33, no. 3, pp. 3181–3188, May 2018.

[54] National Fire Protection Association, "National electrical code," Article 210.19(A)(1), pp. 210–70, 2017.

[55] "Electricity rates by state," Online, Choose Energy, 2023. [Online]. Available: https://www.chooseenergy.com/electricity-rates-by-state/

[56] "Historical dam load zone and hub prices," Online, Electric Reliability Council of Texas (ERCOT), 2022. [Online]. Available: https://www.ercot.com/mp/data-products/data-product-details?id=NP4-180-ER

[57] IBM, "IBM Decision Optimization CPLEX Modeling for Python," Software, 2023. [Online]. Available: https://pypi.org/project/docplex/